LUND UNIVERSITY

DEPARTMENT OF PHYSICS
DIVISION OF PARTICLE PHYSICS

CP violation in QCD, axions and possible connections to dark matter

BACHELOR'S THESIS

Eric E CORRIGAN

1st February 2014

Abstract

The strong CP problem and its solution are treated on the undergraduate level. We first review the theoretical background of symmetry and symmetry breaking in particle physics. The Goldstone model is treated for several simple systems: the linear sigma model, the Higgs mechanism and the interpretation of pions as pseudo-Goldstone bosons in QCD. The problem of lack of CP-violation in strong interactions is explained, and the most popular solution—the addition of an additional $U(1)_{\mathrm{PQ}}$-symmetric field and its quanta, the axion—is presented. The current experimental status of the axion is detailed, including limits set by laboratory and astrophysical searches. Finally, the axion in the context of its possible role as a dark matter (DM) candidate is reviewed, focusing primarily on the theory of axionic cold dark matter and its status. We find that the axion is an appealing solution to the CP problem, and a highly viable candidate for cold dark matter in the Universe.

Foreword

The subject of this review, submitted for the degree of B.Sc., was first suggested to me by my eventual supervisor Torsten. I had taken a particular interest in the $SU(3)$ gauge field theory of the strong interaction, Quantum Chromodynamics; The beautiful and powerful way in which symmetry is used in quantum field theories, and QCD with its intricacies (owing to the high-dimensional and non-Abelian $SU(3)$ gauge group), appeals to me. I wanted to learn more about some aspect of QCD, and the subject of the strong CP problem spoke to me immediately. The subject of this text, while being approached primarily from a particle physics perspective, also has a deep connection with another fascinating field: cosmology. The strong CP problem and dark matter are two majorly important and theoretically compelling issues in modern particle physics and cosmology, and the axion is a natural and elegant solution to both.

My attempt in this text is to explain the strong CP problem, its axion solution, and the viability of the axion as a dark matter candidate on the undergraduate level. These are highly technical subjects; the fact that I have not found any reviews at this level during my study of the literature is probably due to the fact that it is difficult to do these subjects justice without requiring a lot more previous knowledge. With this in mind, the depth of treatment in this review is limited by the knowledge of the intended reader, and in this case, of the author. This means that some things must be (and have been) glossed over. In these cases, I have attempted to give the gist of the arguments, quote the results and refer to full discussions in the literature. I have included a short primer on the Standard Model and the most important discrete symmetries.

It is my opinion that the lack of reviews of this topic at the undergraduate level justifies my attempt. Accessible reviews of theoretically important issues are a major tool for attracting new scientists into the relevant field.

In hindsight, I would have benefited from deeper insight into general quantum field theory in order to better understand the $U(1)$ problem and its solution, calculations and estimates of the dynamics of the axion field, etc. These arguments are often complicated, and the original literature quite impenetrable. Some additional knowledge on the evolution and large-scale structure of the Universe would have been useful for the chapter on DM and cosmology, but the concepts involved here are generally easier to grasp than the more mysterious quantum field-theoretical arguments.

Contents

1 Introduction

1.1 Background and rationale

Symmetries play a vital role in a physicist's understanding of the world, and nowhere more so than in particle physics. The symmetries of parity (P), charge conjugation (C), time reversal (T) and their combinations guide predictions and calculations, while gauge (local phase) symmetries are fundamental in the very construction of new theories. After a short primer in the Standard Model below, we discuss the discrete symmetries in Chapter 2. For a long time, P was believed to be a fundamental, geometrical symmetry in Nature. It is certainly an intuitive picture that if one reverses all spatial dimensions, the fundamental interactions behave the same. However, in the 1950s it was discovered[1] that the weak interaction did not obey this symmetry. Then, it was thought, CP must be the correct fundamental symmetry. Thus, a process in which the spatial dimensions are mirrored and particles exchanged for their antiparticles should be essentially equivalent to the unmirrored version of the process. It came as a big surprise when, in the 1960s, it was found[2] that the weak interaction violates this symmetry too. This was initially a mystery, but we will see why this happens in Chapter 2. In Chapter 3 we examine another important symmetry concept: continuous symmetries, how they are broken, and resulting particles. These models, in addition to being beautiful, will also be important to the main topics of this review.

Now, the strong CP problem, which is the main focus of Chapter 4, is rather of the opposite nature to CP violation in the electroweak sector: Instead of CP being violated for initially unknown reasons, CP is very well conserved in strong interactions, but it is not at all clear why: It turns out that we must add a term which violates CP to the QCD Lagrangian. This term, parametrised by the number θ, is required to solve the so-called $U(1)$ problem, which we also discuss in Chapter 4. This term violates CP, unless the relevant parameter θ is zero. Measurements on the neutron electric dipole moment show that CP is very well conserved, and thus it follows that θ must be very small, which there is no *a priori* reason to expect. This fine-tuning problem is the strong CP problem. The generally favoured solution to this problem was proposed by Roberto Peccei and Helen Quinn [43, 44] in the 1970s. In essence, the Lagrangian is made symmetric under a new $U(1)_{\mathrm{PQ}}$ symmetry, and θ is promoted to a field rather than a constant. The dynamics of this field then tend to relax the parameter to zero. This is treated in Chapter 4. The quantum of this field is the axion, arising as a (pseudo-) Goldstone boson of the broken PQ symmetry. In Chapter 5, following a brief general discussion of dark matter, we examine the viability of the axion as a DM candidate.

[1] Tsung-Dao Lee and Chen Ning Yang were awarded the 1957 Nobel prize for this.

[2] The 1980 Nobel physics prize was given to James Watson Cronin and Val Logsdon Fitch for discovering CP violation.

1.2 The Standard Model

The Standard Model (SM) of particle physics is a Quantum Field Theory (QFT) which describes the fundamental particles of Nature and their interactions, except gravitation. The particles are sectioned into three main groups: leptons, quarks and gauge bosons. The described interactions are subdivided into the unified electroweak (containing the Higgs sector) and strong sectors, where the elecroweak interaction is a combined theory of the weak nuclear and electromagnetic forces. The current theory of the strong nuclear interaction is Quantum Chromodynamics (QCD). The Higgs mechanism is the generator of particle masses.

The SM is usually formulated in terms of Lagrangian densities, $\mathscr{L}$. This is convenient because $\mathscr{L}$ is a single scalar function from which all properties of the theory follow. Starting from the free particle Lagrangians, the interactions of the particle fields are deduced by the requirement that the systems described by the Lagrangian densities (commonly called simply Lagrangians for brevity) are invariant under specific gauge symmetries (which, in other words, leave the equations of motion unchanged). As the behaviour of the Lagrangian under these transformations is known, the behaviours of the new fields, introduced to preserve invariance, can be found. This procedure of 'gauging' a theory is usually performed by replacing the normal derivative ∂_μ with a *covariant derivative* D_μ in the Lagrangian. This introduces new terms which are interpreted as the interactions of the theory. The Lagrangian of a system contains full information about the dynamics; the equations of motion of the system can be found through the principle of stationary action, in complete analogy with classical mechanics.

The gauge group of the electroweak sector is $SU(2) \times U(1)$, while QCD possesses internal $SU(3)$ gauge invariance. Thus, the gauge under which the SM transforms invariantly is $SU(2) \times U(1) \times SU(3)$. Here, invariance under $U(1)$ is phase invariance, and $SU(n)$ is the n-dimensional Special Unitary group. The covariant derivative of the SM is

$$D^\mu = \partial^\mu - ig_1 \frac{Y}{2} B^\mu - ig_2 \frac{\tau_i}{2} W_i^\mu - ig_3 \frac{\lambda_a}{2} G_\alpha^\mu,$$

where $i = 1, 2, 3$, $\alpha = 1, 2, ..., 8$. $g_{1,2,3}$ are (scale dependent) coupling constants. Y, τ_i and λ_a are the generators of transformations in $U(1)$, $SU(2)$ and $SU(3)$ respectively. B, W and G are the electroweak boson and gluon fields (B and W^0 become, upon spontaneous breaking of the electroweak gauge symmetry, the photon and the Z^0 boson—see Section 3). Note that the generators are matrices in general (1x1 for $U(1)$), but that the equation still makes sense as the quantities being operated upon (the boson fields) live in different spaces.

1.2.1 Particle content

The Standard Model contains 12 fundamental fermions, six leptons and six quarks. Additionally, each fermion has a distinct antiparticle with identical mass and conjugated quantum numbers. The leptons are arranged in three doublets (in weak isospin $SU(2)$ space), or *generations*, consisting of one lepton and one corresponding neutrino,

$$\begin{pmatrix}\nu_e\\ e^-\end{pmatrix}, \begin{pmatrix}\nu_\mu\\ \mu^-\end{pmatrix}, \begin{pmatrix}\nu_\tau\\ \tau^-\end{pmatrix}$$

with antiparticles

$$\begin{pmatrix}e^+\\ \bar{\nu}_e\end{pmatrix}, \begin{pmatrix}\mu^+\\ \bar{\nu}_\mu\end{pmatrix}, \begin{pmatrix}\tau^+\\ \bar{\nu}_\tau\end{pmatrix}.$$

The masses obey $m_e < m_\mu < m_\tau$. Neutrino masses were originally zero in SM, but flavour oscillations have been observed, which demand nonzero masses [1]. Neutrino masses can, however, be included into the SM straightforwardly. Neutrino oscillations arise from the fact that the weak eigenstates above are not concurrent with the mass eigenstates, usually labelled $\nu_{1,2,3}$. The fermion masses, including the neutrino upper bounds, are given in Table 1. The electron, tauon and muon all carry electrical charge $-e$ (where e from now on is a positive number), and all neutrinos are uncharged. The charged leptons interact electroweakly, while neutrinos are subject to the weak force only. In SM, leptonic interactions adhere to the concept of *lepton universality*, which means that the only differences between the interactions of the different generations are due to differences in mass. As leptons do not transform between generations (at least in the vanishing neutrino mass limit), we define a conserved lepton quantum number for each generation.

The remaining fermions are the quarks. There are six distinct *flavours*, again grouped into generations:

$$\begin{pmatrix}u\\ d\end{pmatrix}, \begin{pmatrix}c\\ s\end{pmatrix}, \begin{pmatrix}t\\ b\end{pmatrix},$$

and similarly for the antiparticles. Quarks are fractionally charged, with $Q_{u,c,t} = +\frac{2}{3}e$ and $Q_{d,s,b} = -\frac{1}{3}e$. The generations above are ordered from left to right by increasing mass. In addition to the electroweak interactions of the leptons, quarks also interact strongly. Despite great effort, no free quark has ever been observed. This is resolved theoretically by the introduction of the new quantum number *colour charge* and in turn *confinement*. These concepts will be discussed in more detail in the following section on QCD. Quarks combine in bound states as qqq ($\bar{q}\bar{q}\bar{q}$) or $\bar{q}q$. The former state is called a baryon (antibaryon), and the latter a meson. Quarks carry a conserved quantum number called baryon number, $B_q = 1/3$ where q is any quark. This conservation is not fully understood [2]. In addition, each type (or *flavour*) of quark is assigned a quantum number which is conserved in electromagnetic and strong interactions.

Table 1: *SM lepton and quark masses* [21]. *As the listed neutrinos are not mass eigenstates, the limits should be interpreted as mass expectation values of the mixed states.*

Particle	Mass/MeV	Particle	Mass/MeV
e^-/e^+	0.511	$u/\bar{u}$	1.7–3.1
$\nu_e/\bar{\nu}_e$	$< 2 \times 10^{-6}$	$d/\bar{d}$	4.1–5.7
μ^-/μ^+	105	$s/\bar{s}$	80-130
$\nu_\mu/\bar{\nu}_\mu$	< 0.19	$c/\bar{c}$	$(1.18–1.34)\times10^3$
τ^-/τ^+	1780	$t/\bar{t}$	$(4.13–4.85)\times10^3$
$\nu_\tau/\bar{\nu}_\tau$	< 18.2	$b/\bar{b}$	$(172–174)\times10^3$

In the Standard Model, *gauge bosons* mediate the forces. The photon γ mediates the electromagnetic interaction. The $W^\pm$ and Z^0 bosons are the carriers of the weak force. QCD is mediated by gluons g. Gluons each possess a colour and an anticolour charge, which allows them to change the colour states of quarks. For this reason, they also interact strongly themselves. There are eight types of gluons (in general, invariance under $SU(n)$ yields n^2-1 gauge bosons). The SM also predicts one Higgs boson, seemingly discovered [3, 4], whose field spontaneously breaks the electroweak gauge symmetry, which allows nonzero particle masses.

1.2.2 The forces

The electroweak sector contains the unified electromagnetic (described by Quantum Electrodynamics, QED) and weak forces. Its gauge group is $SU(2)\times U(1)$, where it is common to add the subscripts $SU(2)_L$ and $U(1)_Y$. Here, Y denotes the *electroweak hypercharge*, defined as $Q = I_3 + \frac{Y}{2}$, where Q is electric charge and T_3 is the third component of the (weak) isospin. Y is the scalar which generates $U(1)$ gauge transformations. The subscript L indicates that the $SU(2)$ gauge group acts only on left-handed states: the SM treats left- and right-handed particles differently (a theory which has this property is called *chiral*). We represent (using the first generation leptons as an example: a generalisation is straightforward) a right-handed electron e_R^- by a singlet in $SU(2)_L$ space, and left handed electrons and neutrinos by the $SU(2)_L$ doublet

$$\begin{pmatrix} e_L^- \\ \nu_L \end{pmatrix}.$$

In this formulation, the W bosons perform rotations in electroweak isospin space, and thus allow transformations between e_L^- and ν_L. The e_R^- singlet is invariant under these rotations and thus cannot couple to neutrinos. No right-handed neutrinos have ever been detected. The gauge boson fields which

are associated with the $SU(2) \times U(1)$ transformations are B^μ and W_i^μ. B^μ belongs to the weak hypercharge $U(1)_Y$ group, with W bosons $W^\pm$ and W^0 corresponding to $SU(2)_L$. Starting from the leptonic interaction Lagrangian terms we may construct the theory such that it includes the familiar photonically mediated EM interaction, and a new *neutral current* interaction, mediated by the Z^0 boson. The bosons relate as

$$\begin{pmatrix} \gamma \\ Z^0 \end{pmatrix} = \begin{pmatrix} \cos\theta_W & \sin\theta_W \\ -\sin\theta_W & \cos\theta_W \end{pmatrix} \begin{pmatrix} B^0 \\ W^0 \end{pmatrix}$$

where θ_W is the *Weinberg angle*. Neutral current interactions are flavour-conserving. However, *charged current* interactions, mediated by $W^\pm$, do not conserve flavour.

As for leptons, the electroweak quark eigenstates do not coincide with the mass eigenstates. Additionally, if the *d, s, b* quarks participate in charged current interactions through linear combinations of each other,

$$\begin{pmatrix} d' \\ s' \\ b' \end{pmatrix} = \begin{pmatrix} V_{ud} & V_{us} & V_{ub} \\ V_{cd} & V_{cs} & V_{cb} \\ V_{td} & V_{ts} & V_{tb} \end{pmatrix} \begin{pmatrix} d \\ s \\ b \end{pmatrix},$$

the weak interaction will obey quark-lepton symmetry. Here, the mixing matrix V_{ij} is called the Cabibbo-Kobayashi-Maskawa (CKM) matrix.

In the electroweak Lagrangian, mass terms are not invariant under our internal gauge transformations. Thus some additional mechanism must be employed to accommodate particle masses. *Spontaneous symmetry breaking* is the process by which a symmetry is broken for the ground state (vacuum) of a system, but remains valid for the Lagrangian. This is achieved by assigning a nonzero vacuum expectation value (VEV): naïvely, the vacuum would have a vanishing VEV. By introducing a degeneracy into the vacuum state, for example by defining a new field, a particular ground state may be chosen as *the* vacuum state. This arbitrarily chosen vacuum state is no longer invariant under the gauge symmetries of the theory, while interactions with the new field remain so. We say that the original symmetries are spontaneously broken. This concept will be discussed in detail in Section 3. The Higgs mechanism is detailed in Section 3.1.3.

For the electroweak case, let us introduce a new complex scalar *Higgs field*, which permeates space and is a doublet in $SU(2)_L$, with one neutral and one charged component:

$$\phi = \begin{pmatrix} \phi^+ \\ \phi^0 \end{pmatrix}.$$

Now, let ϕ^0 have a nonzero VEV. With this choice, the selected vacuum state will violate the electroweak gauges $U(1)_Y$ and $SU(2)_L$ and instead possess invariance under a new gauge $U(1)_{EM}$, the gauge group of the EM interaction. Hence, the QED gauge boson (the photon) remains massless, and the remaining gauge

bosons (W, Z) acquire mass. This also results in the condition

$$\frac{M_W}{M_Z} = \cos\theta_W,$$

a prediction in terms of the measured mixing angle, in excellent agreement with experiment. The Higgs mechanism can also be made to account for fermion masses by adding interactions between the fermion and Higgs fields.

1.2.3 Quantum Chromodynamics

Quantum Chromodynamics is the gauge theory which describes the strong (colour) interaction. The QCD Lagrangian is

$$\mathscr{L}_{\text{QCD}} = \bar{\psi}_i(i\gamma^\mu D_\mu - m)\psi_i - \frac{1}{4}G^a_{\mu\nu}G^{\mu\nu}_a, \tag{1.1}$$

where the first term is fermionic and the second describes the gauge bosons. ψ is a Dirac spinor with three colour components, while i is a flavour index. G is the gluon field strength tensor, defined as

$$G_{\mu\nu} = \partial_\mu G_\nu - \partial_\nu G_\mu - ig_3[G_\mu, G_\nu].$$

g_3 is the coupling constant and m is the quark mass. γ^μ are the gamma matrices. The gauge group of QCD is $SU(3)_C$. The quarks are assigned to left-handed doublets and right handed singlets in $SU(2)_L$, while being triplets in $SU(3)_C$. Gluons are singlets in $SU(2)_L$ and octets in $SU(3)_C$. We call the $SU(3)_C$ charge *colour*, where the allowed values are to be referred to as red, green and blue (r, g, b). Thus, the conjugated charges allowed for antiquarks are antired, antigreen, antiblue $(\bar{r}, \bar{g}, \bar{b})$. The strong coupling constant g_3 is large at distances $r \geq 1$ fm, and, as we shall discuss, decreases as the momentum transferred by the mediating gluons increases (or as r decreases). As the colour coupling is strong at large distances, perturbation theory (e.g. the Feynman diagram approach) breaks down, as higher order terms become significant. This means that computational methods such as *lattice QCD* must be relied on for predictions. Below, we will discuss two important characteristics of the strong force, *colour confinement* and *asymptotic freedom*.

Confinement Colour confinement is the mechanism through which particles carrying $SU(3)_C$ colour charge are forbidden from existing in isolation, and through which the lack of observed free quarks is explained. Only colour singlets may exist as final quark states. The discussion below is handwaving, as a full explanation requires theory beyond our scope.

We begin by considering the EM interaction as an analogue. The field lines between the charges of an electric dipole are familiar to all students of physics. We may imagine such field lines, now representing the colour field, between two quarks. We shall assume that the interquark distance is $r \geq 1$ fm. Where the EM field lines are allowed to go to infinity, the colour field lines between

two $SU(3)_C$ charges are held together in a tight *flux tube* between the charges. This is due to the fact that, while photons are themselves uncharged (the gauge group is Abelian): the gluons that mediate the colour force self-couple. This self-interaction serves to keep the cross-sectional area of the tube constant with the charge separation. Thus, the energy contained by the gluon field increases linearly with colour charge separation. This is a remarkable result: it implies that separation of one colour charge from the other requires infinite work. This is the origin of confinement. If energy is supplied to the field, eventually it will become energetically favourable to create a new quark-antiquark pair from the vacuum. In high-energy collisions, quarks form jets of hadrons and other particles.

As we have argued, quarks and gluons may only exist in final states as colour singlets (i.e., states invariant under rotations in colour space). One way to do so is the state $\frac{1}{\sqrt{3}}(r\bar{r} + g\bar{g} + b\bar{b})$. These are the meson states, $\bar{q}q$. We may also write $\epsilon_{ijk}q_iq_jq_k$, where ϵ is the Levi-Civita tensor and $i, j, k = r, g, b$: this is the familiar baryon state containing three quarks. Furthermore, more complex colourless *exotic* hadronic states may be formed, such as $qq\bar{q}\bar{q}$ and $qqqq\bar{q}$. These are not forbidden by QCD, but have not been measured as making any large contribution to hadron physics [5]. Additionally, mesons comprised of gluons, *glueballs*, are expected to mix with $q\bar{q}$ states. It can be shown that all colour singlet states have integer electrical charge (if assumed to have baryon number $B \leq 0$) [5].

Asymptotic freedom The strong coupling constant g_3 decreases as the momentum transferred by the mediating gluons increases (or as r decreases). This *running coupling* gives rise to the phenomenon known as *asymptotic freedom*: The force between colour charges weakens with smaller separation. This can be explained by *antiscreening*. We shall illustrate this by first discussing a familiar non-Abelian analogue. In QED, quantum fluctuations can produce $l\bar{l}$ pairs, where l is any charged lepton. These, and higher order diagrams, produce a *vacuum polarisation*: the charge of the virtual particles screens the charge of any real charges in the region. Close to the screened charge the effect is weak, but as distance increases, the effective charge becomes smaller. This is analogue to molecular polarisation in a dielectric. Thus, screening has produced a dependence on distance in the coupling strength. In QCD, there is an analogous effect; here however this effect has extra intricacies: Due to virtual gluons, which carry colour, both screening and *antiscreening* effects are produced. As it turns out, the antiscreening effect dominates normal (colour) screening, and thus we are left with a net antiscreened colour charge. Hence, as we get closer to the charge (or probe it with higher Q^2), it seems weaker. The strong coupling g_3 decreases with increasing probe momentum-squared and decreasing distance. This is asymptotic freedom. Quarks confined inside hadrons are asymptotically free, and as such processes involving closely bound quarks can be undertaken using perturbative methods.

1.2.4 Open issues and challenges

The Standard Model, while being one of the most successful and complete theories in the history of physics, is fundamentally incomplete in some areas, and aesthetically unsatisfactory in others. The following is a short review of some of the most prominent shortcomings of the SM.

- Gravitation. There is, as yet, no known way of satisfactorily including general relativity in the quantum field-theoretic framework of the SM.
- There is a large degree of arbitrariness in the fundamental structure of the particles and forces. Why are there three generations? Why is the gauge group specifically $SU(2) \times U(1) \times SU(3)$?
- There are a large number of parameters which must be specified rather than are predicted. There are *at least* 25: 12 fermion masses, 3 interaction couplings, 8 phases in quark and neutrino mixing and 2 free parameters in the Higgs sector. This is inelegant at best, and ultimately unsatisfying. Some of these closely related parameters span over many orders of magnitude for no apparent reason.
- The SM contains a number of unsolved problems and oddities, such as the matter-antimatter asymmetry, as well as a number of fine-tuning problems such as the *hierarchy problem* of the Higgs mass and the *strong CP problem* (discussed in detail in Section 4.1).

Many of these might be solved by adding to and modifying the SM, e.g. by supersymmetric or extra-dimensional extensions; although it is generally felt [2] that a more fundamental theory is needed.

2 Discrete symmetries

2.1 C, P, T, CP and CPT

For completeness, we will devote some space to the important discrete symmetries C, P and T, even though they are assumed to be familiar to the reader. Further, we will also state the famous and deeply important *CPT theorem* in basic terms. In anticipation of the full discussion of CP invariance in QCD in Chapter 4, we will also briefly discuss CP violation in the electroweak sector of the Standard Model.

2.1.1 Parity (P)

We shall define the parity operation as the reflection $\vec{x} \to -\vec{x}$ of the three spatial coordinates. We also introduce the parity operator $\hat{P}$:

$$\hat{P}\psi(\vec{x}, t) \equiv P\psi(-\vec{x}, t).$$

Here, P is a phase factor. ψ is a one-particle wave function which satisfies the Schrödinger equation. As

$$\hat{P}^2\psi(\vec{x}, t) = \psi(\vec{x}, t),$$

$P^2 = 1$. Considering a momentum eigenstate $\phi \propto \exp(i(\vec{p} \cdot \vec{x} - Et))$, it follows that

$$\hat{P}\phi_{\vec{p}}(\vec{x}, t) = P\phi_{\vec{p}}(-\vec{x}, t) = P\phi_{-\vec{p}}(\vec{x}, t).$$

Thus, in the rest frame of a particle, P is an eigenvalue, and we define the *intrinsic parity* P_a of a particle a by

$$\hat{P}\phi_{\vec{p}=0}(\vec{x}, t) = P_a\phi_{\vec{p}=0}(\vec{x}, t).$$

For the special cases $P_a = \pm 1$ we say that a has even or odd parity, respectively. As usual, if $\hat{P}$ commutes with the Hamiltonian of a system, P is a good quantum number. For a system of particles, the intrinsic parity is the product of the parities of the individual particles. It can be shown that the parity of an antifermion is opposite to that of the corresponding fermion. It is conventional to fix the parities of the SM by defining $P_{e^-} = P_p = P_n = +1$, letting the others follow.

For a many particle state with orbital angular momentum L, we have, for particles $a, b, ...,$

$$\hat{P}\,|a, b, ...; L\rangle = P_aP_b \cdots (-1)^L\,|a, b, ...; L\rangle$$

In the framework of QFT, writing the right- and left-handed projections of a Dirac spinor ψ as

$$\psi_R \equiv \frac{1}{2}(1 + \gamma^5)\psi;$$

$$\psi_L \equiv \frac{1}{2}(1-\gamma^5)\psi,$$

parity transforms between left- and right-handed spinors. As the weak interaction is a chiral theory, it violates parity. Symmetry under parity transformation is exactly conserved in the strong and EM sectors.

2.1.2 Charge conjugation (C)

C-symmetry is symmetry under the operation of charge conjugation: $C \to -C$, applied to all types of charges (generators of continuous symmetries) in the system: essentially replacing each particle with its antiparticle. We will define the C-parity of a system in complete analogy with parity as discussed above. C-parity is a conserved quantity for systems for which C is a symmetry. For a particle-antiparticle (denoted a and $\bar{a}$) state with orbital angular momentum L and total spin S, we obtain

$$\hat{C}\,|a\bar{a};L;S\rangle = (-1)^{L+S}\,|a\bar{a};L;S\rangle$$

Note that the same result is valid for both fermionic and bosonic states, although for slightly different reasons: In both cases, we get a prefactor $(-1)^L$ from the spherical harmonic. For bosons, we also have $(-1)^S$ from the spin part of the wave function. In the fermionic case, there is a prefactor (-1) from fermion-antifermion exchange and $(-1)^{S+1}$ from spin.[3]

In the context of quantum field theory, we can define the charge conjugation operator [6]

$$C = i\gamma_2\gamma_0$$

with the properties $C^\dagger = C^T = C^{-1} = -C$. Here, the γ's are the familiar Dirac matrices and C is basis-independent.

C-symmetry is obeyed in electromagnetic and strong interactions, but violated in weak.

2.1.3 Time reversal (T)

T-symmetry, or symmetry under time reversal is the transformation $t \to -t$. Again, the weak interaction violates T symmetry. It is a symmetry of the EM and strong sectors. We define the time reversal operator $\hat{T}$ by

$$\hat{T}\psi(t,\vec{x}) \equiv \psi^*(-t,\vec{x}).$$

This operator is neither linear nor Hermitian (in fact, it is antiunitary), and thus, in contrast to C and P, the T symmetry of a system does not imply the conservation of a T-parity quantum number. Note that the time reversal operator returns a complex conjugate state. This can easily be seen by the transformation $\mathrm{e}^{iEt} \to \mathrm{e}^{-iEt}$ under T of a plane wave.

Due to the power and generality of the CPT theorem (discussed below), violation of T-symmetry implies CP-violation in all situations of interest to us.

[3] The factor (-1) for fermion-antifermion pairs results from quantum field-theoretic effects which we will not consider in any further detail [5].

2.1.4 CP

CP-symmetry is symmetry under simultaneous C and P operations. CP is violated in the SM, as shall be discussed in detail in the following section. There is direct CP violation in the electroweak sector; however, the strong interaction does seem to obey CP to a high degree, despite absence of any theoretical basis for exact symmetry. This is known as the *strong CP problem*, discussed at length in Section 4.1.

2.1.5 CPT and the CPT theorem

The CPT theorem is a theoretical connection between the properties of Lorentz and CPT invariance. It is regarded an exact symmetry of all interactions, as they are currently formulated. The CPT theorem states that any local quantum field theory, which

- has been quantised in such a way that it satisfies the spin-statistics theorem and
- can be written as a normally ordered Lagrangian, which is Lorentz invariant and Hermitian,

is symmetric under CPT [7, 8]. It can also be shown that the converse is true: If a theory violates CPT, it must also violate Lorentz covariance [9].

Thus, as the CPT theorem has such general requirements regarding the theories for which it holds, any observed CPT violations would be powerful signals of underlying physics. At present, a large amount of data is consistent with CPT and Lorentz invariance in all fundamental interactions [9, 10]. CPT is the only symmetry combined from C, P, T and CP which is fundamentally obeyed in the current understanding of Nature [11].

2.2 CP violations in the Standard Model electroweak sector

In the electroweak sector, there is a small but measured CP violating effect. In neutral K decays, there is an asymmetry between the decays to $\pi^- e^+ \bar{\nu}_e$ compared to $\pi^+ e^- \nu_e$ of the size of 0.003 [12]. Meanwhile, in B decays, a much larger effect of 0.70 has been seen [12]. Both of these effects are due to *indirect* CP violation— asymmetry in the mixing between the $K^0 - \bar{K}^0$ and $B^0 - \bar{B}^0$ states. *Direct* CP violation, that which results purely from decay through forbidden channels, has also been observed, e.g. in the $B \to K^+\pi^-$, $K^+\pi^0$, $\pi^+\pi^0$ decays [13]. The electroweak sector of the SM directly violates CP through the Kobayashi-Maskawa (KM) phase, introduced in the (complex) CKM matrix

$$V = \begin{pmatrix} V_{ud} & V_{us} & V_{ub} \\ V_{cd} & V_{cs} & V_{cb} \\ V_{td} & V_{ts} & V_{tb} \end{pmatrix}.$$

V is unitary, which places several constraints on the elements. We may also freely redefine the quark mass eigenstates, which means V can be parametrised. An example parametrisation is

$$V = \begin{pmatrix} c_{12}c_{13} & s_{12}c_{13} & s_{13}\mathrm{e}^{-i\delta} \\ -s_{12}c_{23} - c_{12}s_{13}s_{23}\mathrm{e}^{i\delta} & c_{12}c_{23} - s_{12}s_{13}s_{23}\mathrm{e}^{i\delta} & c_{13}s_{23} \\ s_{12}s_{23} - c_{12}s_{13}c_{23}\mathrm{e}^{i\delta} & -c_{12}s_{23} - s_{12}s_{13}c_{23}\mathrm{e}^{i\delta} & c_{13}c_{23} \end{pmatrix}.$$

Here we take $c_{ij} = \cos\theta_{ij}$, $s_{ij} = \sin\theta_{ij}$ with the three Euler angles $\theta_{ij} = \theta_{12}, \theta_{13}$ and θ_{23}, which can be assumed to lie in the first quadrant so that $s_{ij}, c_{ij} \leq 0$ [5]. Now, we can see how the phase δ produces CP violation: We saw in Section 2.1.3 that the time reversal operator $\hat{T}$ performs a complex conjugation when operating on a state. Thus, if the phase $\delta \neq 0$, T is not a symmetry. Then, by the CPT theorem stated in Section 2.1.5, CPT must hold and so CP must be violated. As, from experiment, $s_{13} \ll s_{23} \ll s_{12} \ll 1$ [14], the CKM matrix is commonly written in the approximate *Wolfenstein parametrisation*

$$V = \begin{pmatrix} 1 - \frac{1}{2}\lambda^2 & \lambda & A\lambda^3(\rho - i\eta) \\ -\lambda & 1 - \frac{1}{2}\lambda^2 & A\lambda^2 \\ A\lambda^3(1 - \rho - i\eta) & -A\lambda^2 & 1 \end{pmatrix} + \mathcal{O}(\lambda^4),$$

as an expansion in the parameter λ. Now, η is the CP violating parameter. The current value is $\eta = 0.341 \pm 0.013$ [12]. All experimental data is in good agreement with the SM predictions; however, the observed matter-antimatter asymmetry of the Universe, if explained by CP violation [15], requires a much larger effect than what is currently seen [12].

An analogous situation exists in the lepton sector, where the so called PMNS matrix describes the mixing of the neutrino states. This matrix also has a CP violating phase, called the *Dirac phase* δ_{PMNS}. However, due to the experimental difficulties associated with neutrinos, the value of this phase, and consequently the contribution to CP-violation from the lepton sector, is unknown.

3 Symmetry breaking: models and resulting particles

Apart from anomalous symmetry breaking—when a symmetry of a classical theory is broken by quantisation—which we will encounter in Section 4.1, there are two main mechanisms for symmetry breaking in Nature: spontaneous and explicit symmetry breaking (SSB and ESB). In this chapter, we shall focus on these two. We will apply the Goldstone model to systems which obey exact and approximate symmetries, and investigate the physical interpretations and predictions. We will first study a simple system symmetric under a global phase symmetry, and later on light-quark quantum chromodynamics.

We have already mentioned the Higgs mechanism and the spontaneous breaking of the $SU(2) \times U(1)$ gauge symmetry in Section 1.2.2. As we argued, we could circumvent the problem of mass terms in the SM Lagrangian not being gauge invariant by introducing a new scalar field which had nonzero values in the vacuum state. In general, spontaneous symmetry breaking is a rather subtle process by which a symmetry can be violated by the vacuum state of a system, but still obeyed by the interactions (in our case, this means the Lagrangian). The Higgs mechanism is essentially an extension of the Goldstone model, which is applied to gauge-invariant theories. Here, we will demonstrate the Goldstone model for a real scalar field with global phase invariance, and see that this results in massless scalar *Goldstone bosons*. Further, we shall see how *pseudo*-Goldstone bosons arise for theories which have both spontaneous and explicit symmetry breaking. In the next chapter, we will study one pseudo-Goldstone boson in particular: the *axion*.

3.1 The Goldstone model

3.1.1 The linear sigma model

The Goldstone model [16] describes a process by which an initial symmetry of a system is spontaneously broken, and new massless scalar bosons result as excitations. A demonstration is given below for a simple system, invariant under an internal, global, Abelian symmetry.

Consider a complex scalar

$$\phi = \frac{1}{\sqrt{2}}[\phi_1 + i\phi_2]$$

and the Lagrangian

$$\mathscr{L} = [\partial^\mu \phi^*][\partial_\mu \phi] - \mu^2|\phi|^2 - \lambda|\phi|^4,$$

where $\mu^2, \lambda \in \mathbb{R}$ are arbitrary parameters. This is known as the linear sigma model (where we have chosen the number of ϕ fields $N = 2$). The corresponding

Hamiltonian[4] is

$$\mathscr{H} = [\partial^0\phi^*][\partial_0\phi] + [\nabla\phi^*]\cdot[\nabla\phi] + \mu^2|\phi|^2 + \lambda|\phi|^4.$$

The last two terms are simply the potential (density) $\mathscr{V}(\phi)$. Naïvely, we would recognise the term $-\mu^2|\phi|^2$ as a mass term: however, we will resist such interpretations for now and simply view μ and λ as parameters of the potential. As is easily verified, $\mathscr{L}$ possesses global $U(1)$ phase invariance:

$$\phi \to \phi' = \mathrm{e}^{i\alpha}\phi,$$
$$\phi^* \to \phi^{*'} = \mathrm{e}^{-i\alpha}\phi^*.$$

The Goldstone model can be employed to spontaneously break this global symmetry, obtaining a new Lagrangian. Now, let us begin by considering ϕ a classical field. We can immediately put $\lambda > 0$, in order for the field energy to be bounded from below as $\phi \to \infty$. We wish to expand the fields, and find the spectrum of excitations (particles). To do this, the first step is to identify the vacuum states. The first two terms of $\mathscr{H}$ are positive definite. Now, μ^2 can lie in two intervals:

1. $\mu^2 > 0$: $\mathscr{V}$ is now positive definite, and thus we have a *unique* vacuum state at $\phi = \phi_1 = \phi_2 = 0$. As briefly discussed in Section 1.2.2, the vacuum state must be degenerate for spontaneous symmetry breaking to occur, and so, $\mu^2 > 0$ will not work. In this situation, we may regard $\mathscr{L}$ as the Lagrangian of a complex Klein-Gordon field, with $-\mu^2|\phi|^2$ being the familiar mass term (and $\lambda|\phi|^4$ interpreted as a self-interaction term after quantisation [17].) In Figure 3.1, the potential $\mathscr{V}$ is plotted against ϕ_1 and ϕ_2.

2. $\mu^2 < 0$: Here, the vacuum corresponds to a circle in the ϕ_1, ϕ_2 plane,

$$\phi_0 = \left(\frac{-\mu^2}{2\lambda}\right)^{1/2} \mathrm{e}^{i\theta}, \quad 0 \le \theta < 2\pi,$$

as shown in Figure 3.1b, with θ parametrising the circle of minimum potential. Let us define a specific vacuum state along the circle of minimum (i.e. a direction in the ϕ_1, ϕ_2 plane). This is arbitrary, and for simplicity we shall select $\theta = 0$, which means that

$$\phi_0 = \left(\frac{-\mu^2}{2\lambda}\right)^{1/2} \equiv \frac{v}{\sqrt{2}} > 0. \tag{3.1}$$

[4] For any Lagrangian (density) $\mathscr{L}(\phi_r(x), \phi_{r,\alpha}(x))$ with $\phi_{r,\alpha} \equiv \frac{\partial\phi_r}{\partial x^\alpha}$, and the conjugate field defined as $\pi_r(x) \equiv \frac{\partial\mathscr{L}}{\partial\dot{\phi}_r}$, the Hamiltonian (density) is written

$$\mathscr{H}(x) = \pi_r(x)\dot{\phi}_r(x) - \mathscr{L}(\phi_r(x), \phi_{r,\alpha}(x)).$$

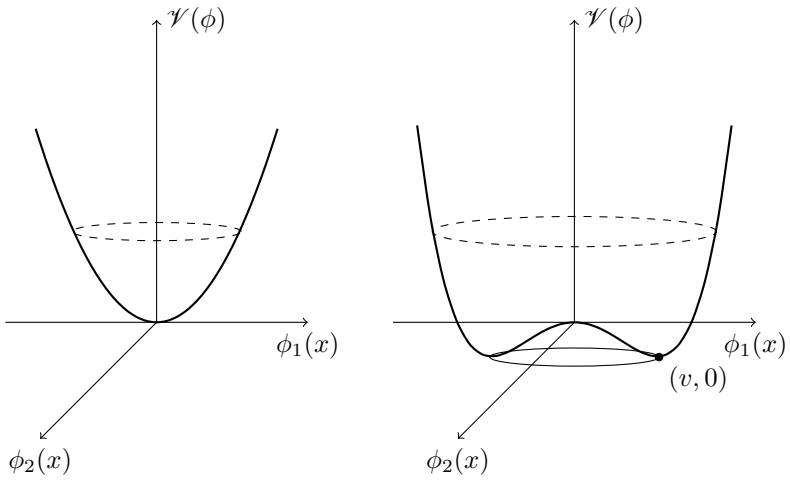

(a) **(b)**

Figure 3.1: *Potential density* $\mathscr{V} = \mu^2|\phi|^2 + \lambda|\phi|^4, \lambda > 0$ *plotted against the complex field* $\phi = 1/\sqrt{2}(\phi_1 + i\phi_2)$. *(a)* $\mu^2 > 0$. *Unique vacuum state with no spontaneous symmetry breaking possible. (b)* $\mu^2 < 0$. *The infinitely degenerate vacuum states lie along the circle with radius* $-\mu^2/\lambda = v$. *Our choice of ground state* $(v, 0)$ *lies on this circle.*

The idea now is to expand around the vacuum state and analyse the resulting Lagrangian. Let us write the field as

$$\phi(x) = \frac{1}{\sqrt{2}}[v + \sigma(x) + i\eta(x)], \tag{3.2}$$

where we have introduced the real fields σ and η. We obtain

$$\begin{aligned}\mathscr{L} = &\frac{1}{2}[\partial^\mu\sigma][\partial_\mu\sigma] - \frac{1}{2}(2\lambda v^2)\sigma^2 + \frac{1}{2}[\partial^\mu\eta][\partial_\mu\eta] \\ &- \lambda v\sigma[\sigma^2 + \eta^2] - \frac{1}{4}\lambda[\sigma^2 + \eta^2]^2 + \text{const.}\end{aligned} \tag{3.3}$$

We shall interpret

$$\mathscr{L}_0 = \frac{1}{2}[\partial^\mu\sigma][\partial_\mu\sigma] - \frac{1}{2}(2\lambda v^2)\sigma^2 + \frac{1}{2}[\partial^\mu\eta][\partial_\mu\eta]$$

as a free Lagrangian and any higher order terms in Equation (3.3) as interactions [17]. Considering $\mathscr{L}_0$, we see that it describes two real Klein-Gordon fields σ and η.[5] The terms containing derivatives of the fields are the usual kinetic

[5]Real Klein-Gordon fields satisfy $(\Box + \mu^2)\phi = 0$ and describe (neutral) spin-0 particles, scalar bosons.

ones: however, we note that while σ has a mass term, with $m_\sigma = \sqrt{2\lambda v^2}$, there is no such corresponding term for η—the η bosons are massless.

We can also take a geometrical view, considering the potential $\mathscr{V}$ (Figure 3.1b), to understand the origin of the masslessness of the η field. To excite the system, we can move in two directions in our (spherically symmetric) potential: either along the circle of minimum, or radially. Radial excitations imply moving from a minimum against the potential, which is increasing quadratically in σ. Such excitations are connected with massive particles. We can also excite the system by moving along the minimal circle in the ϕ plane, but this circle is equipotential and these modes do not result in massive particles [2].

To recapitulate, we have selected one specific degenerate state as *the* vacuum state, obtaining the *vacuum expectation value, VEV*, $\langle\Omega|\,\phi\,|\Omega\rangle = \phi_0 = \frac{1}{\sqrt{2}}v \neq 0$, where $|\Omega\rangle$ is the vacuum. Through this choice the initial global $U(1)$ symmetry of the system has been spontaneously broken, and only in a certain sense does the theory obey the original symmetry: The Lagrangian should still be invariant (in fact it is, though the symmetry is not obvious), but due to our selection of a particular preferred direction in the ϕ plane, the vacuum is not.

3.1.2 Goldstone's theorem

The described process can be generalised into what is commonly called *Goldstone's theorem* [18]: The spontaneous breaking of a continuous symmetry gives rise to massless scalar bosons. These are known as Goldstone bosons (sometimes also as Nambu-Goldstone bosons), and our η bosons are examples of such particles. More technically, we say that the matrix element $\langle G|\,\rho(\vec{x},t)\,|\Omega\rangle$ cannot vanish. Here, $\langle G|$ is the Goldstone boson excitation, $\rho = j^0$ is the density of the Noether charge corresponding to the original symmetry and $|\Omega\rangle$ is the vacuum state [19].[6] The Goldstone bosons must carry the quantum numbers of the conserved currents. There is one Goldstone boson for every generator of the broken symmetry.

We have seen that Goldstone bosons must be massless in a relativistic theory. We could also state this in a different way by saying that Goldstone modes are *gapless*,

$$\lim_{\vec{p}\to 0} E = 0,$$

i.e. the energy of the Goldstone boson must vanish in the limit where its three-momentum vanishes [19].

Finally, it should, of course, be noted that there no pure Goldstone bosons are to be found in Nature, and that any model which includes them as a final result will, as such, be unrealistic.

[6] Recall that Noether's theorem states that, for a field theory, every continuous symmetry of the action of a system implies the existence a current j^μ which is conserved.

3.1.3 Goldstone bosons in gauge theories

The spontaneous breaking of a gauge symmetry is described by the Higgs mechanism. In this section, we shall give a quick recount of this process, for an Abelian gauge symmetry. We will see how the Goldstone bosons appear as additional degrees of freedom in other, massive, bosons.

Consider the Lagrangian

$$\mathscr{L}_{\text{Higgs}} = [D^\mu\phi]^*[D_\mu\phi] - \mu^2|\phi|^2 - \lambda|\phi|^4 - \frac{1}{4}F_{\mu\nu}F^{\mu\nu} \tag{3.4}$$

with covariant derivative $D_\mu = \partial_\mu + iqA_\mu$ and gauge field $F_{\mu\nu} = \partial_\nu A_\mu - \partial_\mu A_\nu$. Our Lagrangian is invariant under the U(1) gauge transformations

$$\begin{aligned}
\phi &\to \phi' = \mathrm{e}^{-iq\alpha}\phi \\
\phi^* &\to \phi^{*'} = \mathrm{e}^{iq\alpha}\phi^* \\
A_\mu &\to A'_\mu = A_\mu + \partial_\mu\alpha
\end{aligned}$$

where α is a function in spacetime. Now, in complete analogy with the discussion in Section 3.1, we take $\lambda > 0$, and spontaneous symmetry breaking can only occur for $\mu^2 > 0$. Here, the vacuum loses its degeneracy through the choice of ϕ_0 in Equation (3.1). Again rewriting the Lagrangian in the new fields η and σ, defined by Equation (3.2), we have

$$\begin{aligned}
\mathscr{L} = &\frac{1}{2}[\partial^\mu\sigma][\partial_\mu\sigma] - \frac{1}{2}(2\lambda v^2)\sigma^2 - \frac{1}{4}F_{\mu\nu}F^{\mu\nu} + \frac{1}{2}(qv)^2A_\mu A^\mu \\
&+ \frac{1}{2}[\partial^\mu\eta][\partial_\mu\eta] + qvA^\mu\partial_\mu\eta + \text{interaction terms} + \text{const.},
\end{aligned} \tag{3.5}$$

where the constant is unimportant as usual and the 'interaction terms' are cubic and higher order in the fields. In interpreting this Lagrangian, we first notice that, as before, we have a real, uncharged scalar Klein-Gordon field σ with mass $m_\sigma = \sqrt{2\lambda v^2}$. However, the term $+qvA^\mu\partial_\mu\eta$ complicates things.[7] We shall instead take a different approach to interpreting the Lagrangian. We start by counting the degrees of freedom in Equation (3.4): There are two in the complex scalar field ϕ and two possible polarisation states for the vector field A_μ.[8] In Equation (3.5), there are two for the real scalars η and σ, but three polarisation states for A_μ. Clearly, then, one degree of freedom is unphysical, as we have only performed algebraic transformations. We can eliminate this degree of freedom by writing

$$\phi' = \frac{1}{\sqrt{2}}(v + \sigma),$$

which is just a gauge transformation [17], under which our system is invariant. Note that we have transformed a complex field ϕ into a real field ϕ'. We will,

[7] This structure of this term in A_μ and η indicates that these fields are not independent and normal [17].

[8] cf. the photon field.

however, redefine and keep calling the transformed field ϕ. Now, substituting, our Lagrangian becomes

$$\mathscr{L} = \mathscr{L}_0 + \mathscr{L}_1,$$

with

$$\mathscr{L}_0 = \frac{1}{2}[\partial^\mu \sigma][\partial_\mu \sigma] - \frac{1}{2}(2\lambda v^2)\sigma^2 - \frac{1}{4}F_{\mu\nu}F^{\mu\nu} + \frac{1}{2}(qv)^2 A_\mu A^\mu$$

and

$$\mathscr{L}_1 = -\lambda v \sigma^3 - \frac{1}{4}\lambda\sigma^4 + \frac{1}{2}q^2 A_\mu A^\mu [2v\sigma + \sigma^2].$$

$\mathscr{L}_0$ can now be treated as a free Lagrangian, describing the real scalar σ with mass $\sqrt{2\lambda v^2}$ and real vector bosons A with mass $|qv|$.

This is the Higgs mechanism. We have moved from a complex scalar field ϕ with a massless vector boson A to a real, massive scalar field σ, and the gauge boson A has been given mass by the spontaneous breaking of the initial gauge symmetry.[9] The massive σ bosons are the Higgs bosons. There are no Goldstone bosons in our spectrum now. Instead, this degree of freedom has been transferred into an additional, longitudinal, polarisation state of the gauge boson (it requires the third polarisation state in order to be massive). This is sometimes referred to in terms of the Goldstone bosons having been 'eaten' by the gauge bosons. Note that this new polarisation state must carry the quantum numbers of the Goldstone boson; i.e. those of the Noether current associated with the generators of the spontaneously broken symmetry.

In the Standard Model, the W and Z bosons each have mass and longitudinal polarisation states due to 'eaten' Goldstone modes, corresponding to spontaneously broken $SU(2) \times U(1)$ symmetry.

3.2 Pseudo-Goldstone bosons

In contrast to spontaneous symmetry breaking, we say that a symmetry is *explicitly* broken when the Lagrangian contains terms which are not invariant. This gives rise to *pseudo-Goldstone bosons*, which are massive, but light. The asymmetric terms in the Lagrangian often make small contributions to the physics of the system, and so we equivalently say that the spontaneous breaking of an approximate symmetry gives rise to pseudo-Goldstone bosons. As an example, let us now review the breaking of the approximate chiral symmetry of QCD and the subsequent appearance of the π mesons as pseudo-Goldstone bosons.

3.2.1 Pseudo-Goldstone bosons in QCD

The masses of the quarks given in Table 1 are the *current algebra*, or free quark, masses. The *constituent masses*, which are the effective masses of bound valence quarks, including contributions from interactions with virtual (*sea*) quarks and gluons, are much larger for the light quarks. In particular, the bare u, d quarks

[9] Note that $m_A = |qv|$ is zero if the vacuum expectation value $v/\sqrt{2}$ is zero.

Table 2: *Masses and quark contents for the lightest hadrons* [21]

Particle	Quark content	Strong isospin	Mass/MeV
$\pi^+(\pi^-)$	$d\bar{u}$ $(u\bar{d})$	1	140
π^0	$u\bar{u},\ d\bar{d}$	1	135
$K^+(K^-)$	$u\bar{s}$ $(s\bar{u})$	1/2	494
$K^0(\bar{K}^0)$	$s\bar{d}$ $(d\bar{s})$	1/2	498
η	$u\bar{u},\ d\bar{d},\ s\bar{s}$	0	548
$\rho^+(\rho^-)$	$u\bar{d}(\ d\bar{u})$	1	775
ρ^0	$d\bar{d},\ u\bar{u}$	1	775

are only around 1% of their constituent masses (which are around 350 MeV [20]). Now, the masses of the lightest hadrons are given in Table 2. As expected on the basis of these facts, even the lightest members of the QCD bound state spectrum are much more massive than the bare u and d quarks. We can use this fact to formulate an approximate symmetry of QCD.

Consider the QCD Lagrangian, Equation (1.1). In the limit $m_u = m_d = 0$, we have

$$\mathscr{L}'_{\text{QCD}} = \bar{\psi}_R(i\gamma^\mu D_\mu)\psi_R + \bar{\psi}_L(i\gamma^\mu D_\mu)\psi_L - \frac{1}{4}G^a_{\mu\nu}G^{a\mu\nu}.$$

This Lagrangian is symmetric under the group G of transformations

$$\begin{pmatrix} u \\ d \end{pmatrix} \to (U_L P_L + U_R P_R)\begin{pmatrix} u \\ d \end{pmatrix}, \tag{3.6}$$

where $P_{L,R} \equiv \frac{1}{2}(1 \pm \gamma^5)$ are the usual Dirac projection operators which produce left and right projections when operating on the Dirac spinors u and d. $U_{L,R}$ are unitary two-by-two matrices with determinant equal to unity [19]. In other words, $G = SU(2)_L \times SU(2)_R$, where the subscripts indicate the handedness of state upon which they act. Just as the electroweak interaction is called chiral because it differentiates between left- and right-handed states (see Section 1.2.2), we say that this is a *chiral symmetry*. It is exact in the massless limit, and approximate when we let m_u and m_d take their real values.

When we consider the hadronic particle spectrum, we see no trace of this symmetry. We would, if the symmetry was approximately respected, expect signs of the hadrons grouping into representations of G, with members of the same multiplet exhibiting approximately degenerate masses. This is not the case. Instead, we note that the lightest mesons in Table 2 are grouped into the representations of $SU(2)_I$—the pions are the isospin multiplet

$$\begin{pmatrix} \pi^+ \\ \pi^0 \\ \pi^- \end{pmatrix},$$

i.e. a triplet in isospin space with third components $I_3 = +1, 0, -1$ respectively. (The following mesons can, in fact, be similarly grouped, now in the larger $SU(3)$ flavour symmetry—kaons into two doublets, η into a singlet, and so on. We will come back to this at the end of the section.)

This means that the approximate symmetry G has collapsed into the subgroup $SU(2)_I$. We can resolve this by noting that G can be made equivalent to $SU(2)_I$ if we let $U_L = U_R$ in Equation (3.6). That is, the approximate symmetry obvious from the groupings in the meson spectrum must result from spontaneous breaking of G in the vacuum state of QCD (resulting in the new approximate symmetry of $SU(2)_I$). Had we wished to be more technical, we would have said that the symmetry G has been dynamically broken by the formation of *quark condensates* in the QCD vacuum—this vacuum structure in turn fails to obey the symmetry of the Lagrangian.

As we saw in the previous section, spontaneously broken symmetries result in massless Goldstone modes. Here, G is not exact, and we only require the masses of the Goldstone bosons to vanish when we move to the $m_u = m_d = 0$ limit. The pions statisfy this requirement. Furthermore, they are pseudoscalar bosons, as required (see Section 3.1.2). It can be shown that they satisfy the other conditions necessary for us to interpret them in this way [19]. For completeness, the corresponding Noether currents are $\vec{j}^{\mu}_L = \frac{i}{2}\bar{\psi}\gamma^{\mu}P_L\vec{\tau}\psi$ and $\vec{j}^{\mu}_R = \frac{i}{2}\bar{\psi}\gamma^{\mu}P_R\vec{\tau}\psi$ for $SU(2)_L$ and $SU(2)_R$ respectively [19]. $\vec{\tau}$ are the Pauli matrices.

Thus, pions are Goldstone bosons in chirally symmetric, two-quark QCD. Goldstone bosons engendered by the spontaneous breaking of an approximate symmetry are known as *pseudo-Goldstone bosons*.

The terms in the theory which explicitly break the symmetry select a preferred direction in the ϕ plane (Figure 3.1b). This process is known as *vacuum alignment*. Thus, the excitations along the previously equipotential circle of minimum will now experience a slightly varying potential (the circle of minimum is tilted with respect to the ϕ_1, ϕ_2 plane), which causes these modes to cost energy, corresponding to small but finite Goldstone masses.

Had we included the third light quark s in our model, so that in the massless limit $m_u = m_d = m_s = 0$, we would instead have been dealing with the spontaneous breaking of an $SU(3)_R \times SU(3)_L$ symmetry. This would have resulted in a final $SU(3)_V$ symmetry (a subgroup) and eight Goldstone bosons. These are in fact the pions, kaons and the η, which form an octet representation of $SU(3)$. This pattern was first seen by Gell-Mann, who called it the Eightfold Way [22]. As the s quark is much heavier than the u and d quarks, $SU(3)$ flavour is a markedly worse symmetry than $SU(2)_I$.

Finally, we note that we could, of course include all quarks in our chiral approximation and end up with an $SU(6)$ flavour symmetry. However, this is pointless in practice, because the enormous masses of the heavy quarks can almost never be neglected at experimental energies.

4 The strong CP problem and axions

We will now begin the treatment of the strong CP problem. We start by introducing the $U(1)$ problem and its solution, which in turn begets the strong CP problem. After a brief look at other proposed solutions, we will describe the generally preferred Peccei-Quinn solution to the problem, and the resulting axion, together with some experimental considerations. Finally, in the next chapter, we will review the axion as a potential dark matter candidate.

4.1 CP violations in QCD: the strong CP problem

4.1.1 The $U(1)$ problem and the θ term

As we saw in Section 3.2.1, the N_f-flavour QCD Lagrangian (1.1) posseses a $SU(N_f)_L \times SU(N_f)_R$ symmetry in the chiral limit of massless quarks. This symmetry is spontaneously broken by the vacuum to isospin $SU(N_f)_I$. This is a good approximate symmetry of Nature, as can be seen from the fact that the states of the hadron spectra (e.g. the meson spectrum in Figure (2)) form multiplet representations of the isospin symmetry. The QCD Lagrangian for massless quarks is actually invariant under further symmetries: There is an exact global $U(1)_B$ symmetry, corresponding to baryon number conservation, which is also experimentally observed. Together, letting $N_f = 2$, $SU(2)_I \times U(1)_B = U(2)_V$ is a predicted and verified approximate symmetry, for the two light quarks u, d. The subscript V stands for vector, which indicates that spinors are transformed independently of chirality (that is, as in our discussion in Section 3.2.1 and Equation (3.6), $U_L = U_R$).

This symmetry is in fact part of a larger symmetry of QCD in the massless quark limit: $U(2)_V \times U(2)_A$. While, as we have seen, the vectorial part is realised in Nature, the axial part consisting of $SU(2)_A \times U(1)_A$ is not. Here, $SU(2)_A$ denotes axial transformations, i.e. of the type of Equation (3.6) with $U_L = U_R^\dagger$. $U(1)_A$ is an exact axial symmetry of the classical theory:

$$\psi \to \psi' = \mathrm{e}^{i\alpha\gamma^5}\psi, \qquad \bar{\psi} \to \bar{\psi}' = \mathrm{e}^{i\alpha\gamma^5}\bar{\psi} \tag{4.1}$$

Such a symmetry is not, however, observed in experiment. We might now assume it has been spontaneously broken; but no suitable pseudo-Goldstone bosons (in addition to the light pseudoscalar mesons discussed in Section 3.2.1) can be found in the hadron spectrum[10]. We conclude that the symmetry has been broken purely by the quantisation of the theory. This is called an *anomaly*. More technically, a theory is said to have an anomaly when there exists no regularisation method which preserves all symmetries of the classical theory.

The issue of the anomalous breaking of the $U(1)_A$ symmetry, and the missing Goldstone boson associated with its generator, is called the $U(1)$ *problem*.

[10] It can be shown that the mass of the corresponding Goldstone mode should be less than $\sqrt{3}m_\pi \approx 240$ MeV [25].

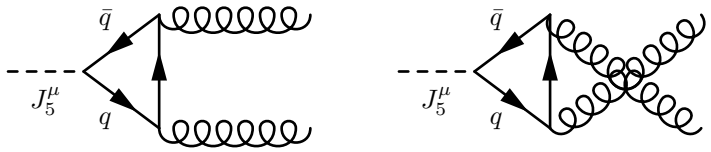

Figure 4.1: *Leading-order diagrams providing nonzero contributions to the divergence of the axial current. The dashed incoming line signifies insertion of the axial current J_5^μ. Quarks run in the loop and connect the current to gluon fields.*

4.1.2 Resolution of the $U(1)$ problem and the QCD vacuum angle

The solution to this problem essentially lies in postulating a more complicated QCD vacuum structure than we naïvely would have. If $U(1)_A$ was indeed obeyed, the associated Noether current

$$J_5^\mu = \sum_q \bar{q}\gamma^\mu\gamma^5 q,$$

where the sum is over light quarks, would be conserved: $\partial_\mu J_5^\mu = 0$. This is indeed what happens at tree level, where this divergence is proportional to the (vanishing) quark masses. However, it turns out that the divergence picks up quantum corrections from cyclic Feynman diagrams, of which the most famous is the so-called *triangle graph*, shown in Figure 4.1. This is called the *Adler-Bell-Jackiw anomaly*, and was first identified in the context of QED, where, among other things, graphs equivalent to those in Figure 4.1 were shown to contribute in $\pi^0 \to \gamma\gamma$ decays [27, 26]. The divergence for our axial current in QCD becomes [30]

$$\partial_\mu J_5^\mu = \frac{g_S^2 N_f}{32\pi^2} G_a^{\mu\nu}\widetilde{G}_{\mu\nu}^a,$$

where $G_a^{\mu\nu}$ is the gluon field strength and $\widetilde{G}_{\mu\nu}^a = \frac{1}{2}\epsilon_{\mu\nu\alpha\beta}G^{a\alpha\beta}$ is its dual. This might appear to have explained the $U(1)$ problem: As the divergence of the current obtains nonzero quantum corrections, and thus fails to be conserved, there is no mystery surrounding the 'missing' Goldstone boson. However, as it turns out, there are further complications: The quantity $G_a^{\mu\nu}\widetilde{G}_{\mu\nu}^a$ can be shown to be a total derivative [31],

$$G_a^{\mu\nu}\widetilde{G}_{\mu\nu}^a = \partial_\mu K^\mu,$$

where

$$K^\mu = \epsilon^{\mu\alpha\beta\gamma}A_{a\alpha}\left(G_{a\beta\gamma} - \frac{g_S}{3}f_{abc}A_{b\beta}A_{c\gamma}\right)$$

is another current. Here, A_a^μ are the gluon gauge fields and f_{abc} are the QCD structure constants. This is remarkable because Lagrangians which differ by

total derivatives are physically equivalent.[11] If the anomaly does not contribute to the action, the system will still be invariant under $U(1)_A$, and we will have our problem back. A closer inspection of the contribution of the anomaly to the action is warranted. The relevant quantity is the integral

$$\delta S \propto \int \partial_\mu J_5^\mu \, \mathrm{d}^4x \propto \int G_a^{\mu\nu} \widetilde{G}^a_{\mu\nu} \mathrm{d}^4x = \int \partial_\mu K^\mu \, \mathrm{d}^4x = \int K^\mu \, \mathrm{d}S_\mu,$$

where the last equality follows from the divergence theorem (the last expression being a surface integral). Here is it clear that, if we take the naïve choice of $A_\mu = 0$ at spatial infinity, the contribution to the action will be zero. However, these are not the correct boundary conditions: The appropriate choice is to take A_μ as a *pure gauge field*. This means that A at spatial infinity should be 0, *or a gauge transformation of 0* [28, 29]. This allows for field configurations called *instantons* such that the integral above is nontrivial.[12] Instantons (sometimes referred to as *pseudoparticles*) are classical solutions to the equations of motion, in Euclidian spacetime (rather than Minkowski space), with finite action [32]. Instantons describe tunneling effects between the different vacua of a theory, effects which cannot be predicted by any perturbative method. In the Yang-Mills theories of interest to us, these distinct vacua can be labelled by a quantum number n, the *winding number*, which can be written [30, 33]

$$n = \frac{ig_s^3}{24\pi^2} \int \mathrm{d}^3x \, \mathrm{Tr}(\epsilon_{ijk} A_n^i A_n^j A_n^k).$$

As each vacuum is characterised by a distinct winding number, we can refer to them as *n-vacua*, $|n\rangle$. As the vacua are degenerate, and instantons allow transitions between them, the physical vacuum state must be written as a superposition of the n-vacua. In fact, it is [30, 32, 35]

$$|\theta\rangle \propto \sum_n \mathrm{e}^{-in\theta} \, |n\rangle \, ,$$

called the *θ-vacuum*. θ is an unknown, 2π-periodic number referred to as the *vacuum angle*. Note that the θ vacuum is the Fourier transform of the n-vacua. There is also an important distinction to make between the n- and θ-vacua: the parameter n specifies different degenerate vacuum states of the same theory, connected by instanton tunnelling. However, the θ-vacua each belong to *different theories*, and transitions between the states cannot be made.

Let us summarise: In order to resolve the $U(1)$ problem, we have been led to a much more complicated QCD vacuum structure than we initially expected. By

[11] Any total derivative added to $\mathscr{L}$ will, upon integrating to obtain the action S, contribute terms which are constant in the generalised coordinates. Thus, when setting $\delta S = 0$, we obtain the same equations of motion.

[12] For a detailed discussion of instanton physics, a working knowledge of the path integral formulation of quantum field theory is recommended, along with some familiarity with the mathematics of topology. This is beyond the scope of this text; we will just outline some major points. For a full discussion, see e.g. Reference [32].

the reasoning above, culminating in the vacuum $|\theta\rangle$, we have successfully allowed for nonvanishing contributions, by the anomalous current, to the action. Thus, $U(1)_A$ is in no way a symmetry of QCD, and we no longer expect a thereto associated preserved Noether current or Goldstone mode. The $U(1)$ problem has indeed been solved. However, to recreate the θ-vacuum structure, we must supply, in the QCD Lagrangian, a term [30, 34]

$$\mathscr{L}_\theta = \theta \frac{g_S^2}{32\pi^2} G_a^{\mu\nu} \widetilde{G}^a_{\mu\nu}$$

The operator $G\widetilde{G}$ violates P (and T), but obeys C, so it violates CP. There is no experimental indication of CP violation in strong interactions: As we shall see in Section 4.1.3, to conform to experimental limits, $\theta \lesssim 10^{-10}$. This is a serious issue: Nothing in the above discussion would lead us to expect such a small value.

This is the *strong CP problem*: Why is the vacuum angle θ, naïvely $\mathcal{O}(1)$, so astonishingly small? Equivalently, why do strong interactions preserve CP to such an exact degree when there is ample opportunity (in the $\mathscr{L}_\theta$ term) for them to do otherwise?

Actually, the vacuum angle picks up contributions both from QCD (as discussed above) and the electroweak sector: Chiral transformations of the type (4.1) generally shift the value of θ [36], and upon the inclusion of weak interactions and the necessary diagonalisation of the quark mass matrix $\mathcal{M}$ (involving a chiral transformation), we gain a contribution to the vacuum angle of size $\arg\det\mathcal{M}$ [30]. Stated differently: We can, through this link, change the value of θ by rotating and redefining the quark fields. Hence, the total physical vacuum angle becomes

$$\bar{\theta} = \theta + \arg\det\mathcal{M}. \tag{4.2}$$

4.1.3 The neutron EDM: predictions and experiment

Before considering possible solutions to the strong CP problem, we will discuss evidence for the smallness of $\bar{\theta}$ and its experimental limits. The primary source of such limits is measurements on the electric dipole moment (EDM) of the neutron. While searches for nonzero permanent EDMs are ongoing for leptons and other particles, the neutron is an ideal system in which to look for such an effect: It has no charge, it is relatively stable, and it is easy to handle as well as produce.

Now, a particle with nonzero permanent EDM necessarily violates CP. To see this, consider a neutron with magnetic dipole moment (MDM) $\vec{\mu}$, spin $\vec{s}$ and hypothetical electric dipole moment $\vec{d}$ aligned as in Figure 4.2. As the only vector available to characterise other properties is the spin, both moments must lie along $\vec{s}$. Spin transforms as $\vec{s} \to \vec{s}$ under parity and as $\vec{s} \to -\vec{s}$ under time

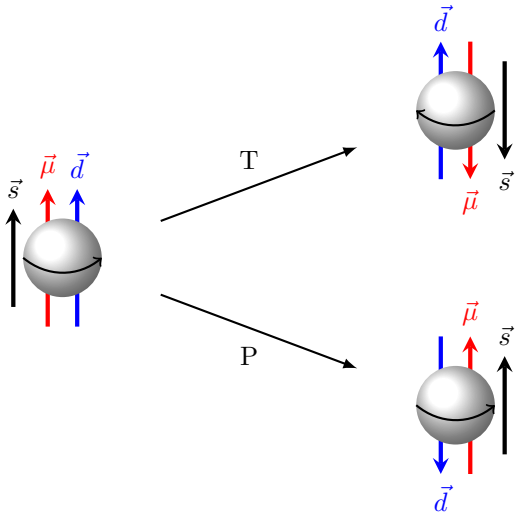

Figure 4.2: *Spin projection, MDM and EDM of a particle under P and T transformations. As* $\vec{s}$ *is the only defining vector along which other quantities can be aligned, the discrepancies between directions of* $\vec{s}$ *and* $\vec{d}$ *under T and P transformations imply that a nonzero net EDM violates these symmetries. Note that* $\vec{\mu}$ *does not suffer from this problem.*

reflection.[13] As we see, $\vec{\mu}$ transforms as $\vec{s}$ under both transformations, and a nonzero magnetic dipole moment is hence allowed under both symmetries. The EDM $\vec{d}$, however, transforms oppositely to the spin in both cases; classically, $\vec{d} = \int_V \vec{x}\rho(\vec{x})\mathrm{d}^3\vec{x}$, which is T-even and P-odd. Thus, the EDM violates T and P. Considering the interaction Hamiltonian

$$H_d = -d\vec{s}\cdot\vec{E},$$

with $d = |\vec{d}|$, it is clear that there is a sign change in H_d under both T and P. By the CPT theorem stated in Section 2.1.5, a (T-violating) nonzero permanent EDM of a particle also violates CP.

We can also simply make the observation that the system with aligned EDM and MDM is not symmetric under either P or T: Under both transformations, initially parallel vectors end up antiparallel, and symmetry is violated.[14]

Let us now discuss how the neutron obtains its electric dipole moment from the QCD vacuum angle. In essence, the neutron EDM arises from a CP-violating coupling to stable hadrons, which allows diagrams of the type displayed in Figure

[13] This is easily seen for orbital angular momentum $\vec{J} = \vec{r}\times\vec{p}$, where $\vec{r}$ is odd under P and even under T, and $\vec{p}$ is odd under both P and T.

[14] We should note that there are systems which can, in fact, have nonzero permanent EDMs; e.g. polar molecules. We shall not pursue this topic, but merely state that there are mechanisms through which these EDMs can be allowed (by, among other things, the system having

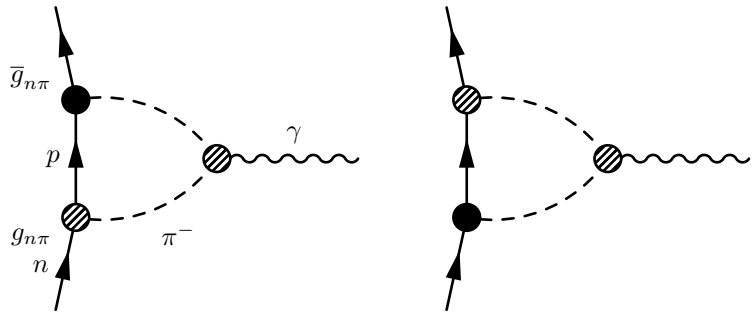

Figure 4.3: *Two diagrams showing the new CP-violating coupling of neutrons to pions, the leading contribution to the neutron EDM. The shaded blobs are the normal, CP-conserving interactions. The black blobs signify CP-violating vertices with coupling* $\bar{g}_{n\pi}$.

4.3. The neutrons disassociate into intermediate hadron states, and the loops constitute a charge separation. Thus, our task is to find the form of the CP-violating hadronic coupling and from this estimate the size of the EDM. This can been done using several methods and models: We will briefly detail one such attempt, the *current algebra* calculations of Crewther et al. [38], and cite the results of a few other works.

We begin by presenting an effective Lagrangian which allows CP-violating interactions. A full derivation of this Lagrangian is beyond the scope of our study, so we will just give a basic outline. Derivations of the Lagrangian and an equivalent Hamiltonian can be found in [38] and [39] respectively, and in the recent review [36].

We will work with three light quarks u, d, s, and seek a CP-violating contribution to the theory $\delta\mathscr{L}_{\text{CP}}$, treated as a perturbation. A critical point to realise in the derivation of $\delta\mathscr{L}_{\text{CP}}$ is that there is, as per Equation (4.2), a connection between the phase of the complex quark mass matrix $\mathcal{M}$ and θ. We can use this fact to rotate out the θ dependence in the Lagrangian, transferring it to $\mathcal{M}$, while retaining the *physical* angle $\bar{\theta}$. This implies that if one of the quark masses vanishes, the mass matrix phase can also be made to vanish (as we can transfer all phases to one quark mass term), and any CP-violation should disappear from the theory. We will return to this briefly in the following section. Here, the main implication is that you cannot simply choose $\delta\mathscr{L}_{\text{CP}}$ as a CP-violating (complex) part of the mass Lagrangian. Instead, you choose a perturbation containing "unitary-equivalent quark-mass terms" [39]. The assumption that the shift in vacuum energy caused by $\delta\mathscr{L}_{\text{CP}}$ is minimal, places sufficient constraints on $\delta\mathscr{L}_{\text{CP}}$ to allow for a parametrisation to be made.

degenerate ground states), violating P while obeying T. See for example [37]. In any case, this cannot be applied to a system like the neutron.

It can then be shown that, assuming $|\bar{\theta}| \ll 1$ and to leading order, we can write [39]

$$\delta\mathscr{L}_{\text{CP}} = \mp \frac{3m_u m_d m_s}{m_u m_d + m_u m_s + m_d m_s} \bar{\theta}(\bar{\psi} i\gamma_5 \psi) \tag{4.3}$$

where the ψ fields are the quarks.

Now, let us review a calculation of the neutron electric dipole moment, made within the framework of current algebra by R.J. Crewther, P. Di Vecchia, G. Veneziano and E. Witten in 1979 [38]. We will try to cover the main points in an understandable way, but much of the underlying theory is beyond our level. For full considerations and derivations, see the original text and references contained therein.

As mentioned earlier, we wish to write the CP-violating $n\pi$ interaction. We will use the effective Lagrangian

$$\mathscr{L}_{n\pi} = \vec{\pi} \cdot \bar{n}\vec{\tau}(i\gamma_5 g_{n\pi} + \bar{g}_{n\pi})n$$

where we have introduced the CP-violating coupling $\bar{g}_{n\pi}$ alongside the usual CP-even coupling $g_{n\pi}$. As usual, $\vec{\tau}$ are the Pauli matrices. $\vec{\pi}$ are the pion fields. Evaluating the amplitude $\langle \pi^a n| \, \delta\mathscr{L}_{CP} \, |n\rangle$ (for some $a \in \{1, 2, 3\}$) yields the result

$$\bar{g}_{n\pi} = -\bar{\theta} \frac{(m_\Xi - m_n) m_u m_d}{F_\pi (m_u + m_d)(2m_s - m_u - m_d)},$$

or $|\bar{g}_{n\pi}| \approx 0.038 |\bar{\theta}|$ [38]. F_π is the pion *decay constant* and the masses m follow an obvious notation.

Evaluation of the neutron dipole moment requires summing over processes containing intermediate stable-hadron states,

$$|X\rangle = |n\rangle \, , |n\pi\rangle \, , |n\pi\pi\rangle \, , \ldots ,$$

of which the pion loops in Figure 4.3 are examples. It turns out that these pion states $|n\pi\rangle$ are the most important (in the small mass limit). An intuitive argument is as follows: As the lightest hadrons, the pions achieve the greatest physical separation during disassociation. This means that this contribution dominates the EDM.

The final step of the calculation is to compute the one-loop diagram (see Figure 4.3) amplitude. The result is

$$d_n = g_{n\pi} \bar{g}_{n\pi} \frac{\ln(m_n/m_\pi)}{4\pi^2 m_n} = 5.2 \cdot 10^{-16} \cdot \bar{\theta} \; e \text{ cm}, \tag{4.4}$$

which should be taken as an order-of-magnitude estimate, due to fundamental limitations of current algebra: The mass ratio in the factor $\ln(m_n/m_\pi)$ in the above expression does not have to be correct; there are other appropriate choices in the $m_\pi \to 0$ limit. The differences between such choices are finite terms, which current algebra methods have no handle on [38].

A slightly earlier calculation by V. Baluni [39] is also of interest. The same (up to normalisation) Lagrangian $\delta\mathscr{L}_{\text{CP}}$ (Eqn. (4.3)) is used, but the rest of the calculations are done using the *MIT bag model*[15]. The result is, using the normalisation of Crewther et al.,

$$d_n = 2.7 \cdot 10^{-16} \cdot \bar{\theta}\ e \text{ cm}. \tag{4.5}$$

More recently, M. Pospelov and A. Ritz [40] performed a calculation of d_n using *QCD sum rules*, achieving

$$d_n = 2.4 \cdot 10^{-16} \cdot \bar{\theta}\ e \text{ cm} \tag{4.6}$$

Clearly, there is very good agreement despite sharp differences in modelling. To acquire limits on $\bar{\theta}$, let us examine current experimental limits on the nEDM.

No neutron electric dipole moment has ever been measured. We shall review a recent experiment, undertaken at Institut Laue-Langevin by Baker et al. (2006) [41], setting the best current limit on the nEDM and $\bar{\theta}$ (the same experiment is also described in [42]). This paper is mainly concerned with theoretical aspects, but a brief discussion on the experimental setup is in order. A schematic is shown in in Figure 4.4. Modern nEDM experiments use *ultracold* neutrons (UCNs); i.e. neutrons with very low energies. The experimental technique most commonly used consists of confining UCNs in cavities containing homogeneous magnetic and electric fields and measuring the *Larmor frequency*; the frequency at which the spin precesses about the field vectors. Consider a neutron with magnetic and electric dipole moments μ_n and d_n, and external electric and magnetic fields $\vec{E}$ and $\vec{B}$. The potential energy contributions are $-\vec{d_n} \cdot \vec{E}$ and $-\vec{\mu}_n \cdot \vec{B}$. We can now write, with Larmor frequency ν, the energy for parallel fields

$$h\nu_{\uparrow\uparrow} = |2\mu_n B + 2d_n E|,$$

and for antiparallel fields

$$h\nu_{\downarrow\uparrow} = |2\mu_n B - 2d_n E|.$$

From this, it is clear that measuring the shift $\nu_{\uparrow\uparrow} - \nu_{\downarrow\uparrow}$ gives us a handle on d_n. At the ILL experiment, spin-polarised UCNs were injected into a cell permeated by a large electric field. The neutrons were then exposed to an oscillating magnetic field (of the order μT). By periodically counting the number of neutrons in either spin state, the neutron transition frequency ν_n could be measured: When the frequency of the B field matched the Larmor frequency of the neturons, a resonant peak in the number of neutrons still in the inital (prepared) spin state was seen.

By simultaneously keeping Hg atoms in the trap, calculating ν_{Hg} and using the relation

$$\frac{\nu_n}{\nu_{Hg}} \approx \left|\frac{\gamma_n}{\gamma_{Hg}}\right| + \frac{d_{\text{meas}}}{\nu_{Hg}} E$$

[15] Quarks are confined to an elastic cavity, or 'bag'. They are treated as light but massive inside, and are allowed to propagate, interacting only weakly. Outside they have infinite mass.

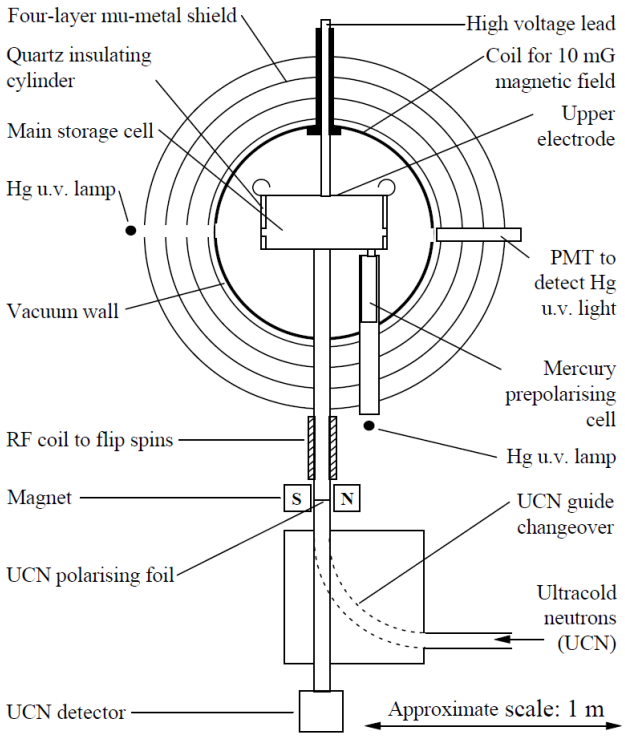

Figure 4.4: *Schematic overview of the ILL nEDM experiment [42]. Polarised UCNs are injected into the 20-litre storage cell, which is shielded against external magnetic field fluctuations. Here, the neutrons are subjected to a constant electric field, and an oscillating magnetic field for a ∼2 s duration. The neutrons are then dropped through a polarising foil which enables counting of the two spin polarisations.*

the measured EDM $d_{\text{meas}} = d_n + |\gamma_n/\gamma_{Hg}|d_{Hg}$ can be obtained [42]. Here, the γs are the gyromagnetic ratios[16].

There are several systematic errors in play, the most important of which were the leakage of a small dipole field into the door cavity and shifts in ν by incident light from the photon beam used to probe the Hg atom precession [41, 42].

The results of these measurements, due to the combined consideration of several analytical approaches, are

$$|d_n| < 2.9 \cdot 10^{-26}\ e\ \text{cm}$$

with 90% CL [41].

[16]The gyromagnetic ratio of a particle is simply $\vec{\mu}/\vec{s}$.

From this limit, and the results in Equations (4.4), (4.5) and (4.6), we see that $\bar{\theta}$ can, at the largest, be of order 10^{-10}.

4.2 Resolving the strong CP problem: $U(1)_{\mathrm{PQ}}$ and the axion

Here, we shall see how the problem detailed above may be resolved. There have been several attempts at resolving this issue. We shall first briefly account for some proposed, but not universally accepted, solutions to the strong CP problem. After this we move on to the most popular approach, due to Peccei and Quinn [43, 44], of introducing a new, spontaneously broken $U(1)_{\mathrm{PQ}}$ symmetry of nature, with its corresponding Goldstone boson, the axion.

As a first example, let us consider at least one massless quark as a solution (here, we mean the 'bare' current algebra masses—the constituent masses are obviously nonzero). As we saw in section 4.1, the value of θ can be shifted by chiral transformations: There is a deep connection between the phases of the quark mass matrix and θ (Equation (4.2)). The consequence of this is that if any quark is massless, any dependence on θ in the theory can be rotated away (the θ-vacua become physically equivalent). However, zero quark masses are not in good agreement with current algebra calculations; even if that were the case, it would not be clear why this bare mass should be exactly zero.

A second class of possible solutions might be constructed by taking CP as a spontaneously broken symmetry: If the fundamental theory is CP-conserving, one can imagine that the observed CP violation in the SM, caused by spontaneous breaking, could generate both the required CP-violating phase and $\bar{\theta} = 0$. Many of these models [45], while successfully achieving the above, require rather disturbing features, e.g. complex Higgs VEVs, which cause further problems. There are, however, more modern models that lack these issues [46]. As an interesting sidenote, R. Peccei writes in his review [30], "In my view, however, the biggest drawback for this solution to the strong CP problem is that experimental data is in excellent agreement with the CKM Model- a model where CP is explicitly, not spontaneously broken."

The Peccei and Quinn solution is, in essence, quite simple. Let us assume that the SM Lagrangian is invariant under a new global chiral $U(1)_{\mathrm{PQ}}$ symmetry. This symmetry is spontaneously broken, generating a Goldstone boson called the axion[17], as first realised by F. Wilczek [47] and S. Weinberg [48]. In essence, the vacuum angle is promoted from a static parameter to a dynamical field. When the effective potential of the axion is minimised, the $\bar{\theta}$ dependence cancels, and the CP problem is no more. We shall see in detail how this comes about.

[17] The axion is probably the only hypothetical particle named after a laundry detergent [49].

We will start by writing a Lagrangian which is invariant under the new $U(1)$ symmetry:

$$\begin{aligned}\mathscr{L} &= \mathscr{L}_{\text{SM}} + \mathscr{L}_{\bar{\theta}} + \mathscr{L}_a \\ &= \mathscr{L}_{\text{SM}} + \bar{\theta}\frac{g_S^2}{32\pi^2}G_b^{\mu\nu}\widetilde{G}^b_{\mu\nu} - \frac{1}{2}\partial_\mu a \partial^\mu a + \mathscr{L}_{\text{int}} + \xi\frac{a}{f_a}\frac{g_S^2}{32\pi^2}G_b^{\mu\nu}\widetilde{G}^b_{\mu\nu} \\ &= \mathscr{L}_{\text{SM}} - \frac{1}{2}\partial_\mu a \partial^\mu a + \mathscr{L}_{\text{int}} + \left(\bar{\theta} + \xi\frac{a}{f_a}\right)\frac{g_S^2}{32\pi^2}G_b^{\mu\nu}\widetilde{G}^b_{\mu\nu} \end{aligned} \tag{4.7}$$

$\mathscr{L}_a$ is the Lagrangian of the new axion field. It contains, apart from the usual kinetic term, some interaction Lagrangian $\mathscr{L}_{int}$ to be adressed later. The parameter f_a is the axion decay constant, which we will also come back to shortly. The last term must be added in order to ensure that the Noether current associated with our new symmetry also has the expected chiral anomaly (see Section 4.1.2)

$$\partial_\mu J^\mu_{\text{PQ}} = \xi\frac{g_S^2}{32\pi^2}G_b^{\mu\nu}\widetilde{G}^b_{\mu\nu},$$

where ξ is a coefficient. The axion a is a real (pseudo-) scalar, which transforms as

$$a \to a + \alpha f_a$$

under $U(1)_{\text{PQ}}$. From the above and Equation (4.7), we see that an axial transformation which shifts a can remove the $\bar{\theta}$ dependence of the theory: This is very important, as it means that the physical vacuum angle is actually $\bar{\theta} + \xi\langle a\rangle/f_a$, where $\langle a\rangle$ signifies the VEV of a, and f_a is now the scale of the spontaneous breaking of the $U(1)_{\text{PQ}}$ symmetry.

Now, due to the nontriviality of the vacuum, as discussed in Section 4.1.2, we also have explicit breaking of the PQ symmetry: The axion becomes a pseudo-Goldstone boson and picks up a small mass. This also means that the axion gains a nontrivial effective potential. Let us consider a potential of the kind discussed in Section 3.1 and Figure 3.1b. If we were to neglect the nontrival vacuum structure—i.e. the instanton effects—the circle of minimal potential would be parallel to the plane, with degenerate ground states, and all values $0 \leq \xi\frac{\langle a\rangle}{f_a} \leq 2\pi$ allowed. In this situation, we have spontaneous breaking of the PQ symmetry. Now, taking the instanton effects into account, the circle of minimum becomes tilted, and we have explicit symmetry breaking, generating axion mass $m_a \neq 0$, and the mechanism through which the $\bar{\theta}$ term can be eliminated from the theory.

We seek now to minimise the potential V_{eff} to see how this happens. It is periodic in the vacuum angle, as we would expect from the above, and quite complicated. However, to leading order, we have [30]

$$V_{\text{eff}} \propto \cos\left(\bar{\theta} + \xi\frac{\langle a\rangle}{f_a}\right).$$

Clearly, this is stationary when the argument = 0. Peccei and Quinn [44] showed that 0 (and not π) is, in fact, the correct choice. Hence,

$$\bar{\theta} + \xi \frac{\langle a \rangle}{f_a} = 0 \quad \Leftrightarrow \quad \langle a \rangle = -\frac{f_a}{\xi} \bar{\theta},$$

and as the axion field evolves, and the potential minimum is reached, the CP violating term from the Lagrangian (4.7) is removed. The strong CP problem is solved. What has happened is that we have essentially switched the fixed parameter $\bar{\theta}$ for a dynamical variable with a CP-conserving minimum, the axion field. As the field evolves, it effectively relaxes the CP-violating term to 0.

4.2.1 Axion dynamics and models

As we shall see, the scale f_a of the spontaneous breaking of PQ symmetry is also the characteristic parameter of the mass and interactions of the axion. Initially, this was assumed to be close to the scale of the electroweak SSB $v_{\mathrm{F}} \approx 250$ GeV, but since axions at this scale have been experimentally excluded (see Section 4.3.1), f_a is now thought to lie much higher. These light, weakly interacting axions are known as 'invisible', and, as dark matter candidates, they will be the main focus of our discussions. There are two main classes of such invisible axion models: the *KSVZ* (Kim-Shifman-Vainshtein-Zakharov)-type and *DFSZ* (Dine-Fischler-Srednicki-Zhitnitsky)-type models. We shall, after a brief introduction to the standard axion properties, review both types. In the following, we shall refer to the physical axion field $a_{\mathrm{phys}} = a - \langle a \rangle$ simply as a.

Standard axion We will first discuss the standard PQWW (Peccei-Quinn-Weinberg-Wilczek) axion. Here, the scale f_a of spontaneous breaking of $U(1)_{\mathrm{PQ}}$ is close to that of $SU(2)_L \times U(1)_Y$. In order to make the SM invariant under the PQ symmetry, the Higgs sector must be expanded to contain at least two scalar field doublets; this minimal model introduces exactly two, Φ_1 and Φ_2. Both Higgs fields have nonzero VEVs; one of the Goldstone modes is eaten by the Z^0, and the axion appears as a Goldstone boson of the PQ symmetry. The axion is the phase field of the Higgs fields. Subsequently, the effective potential due to instantons generates an axion mass (actually, the QCD instanton effects cause mixing of the axion with the (obviously massive) pseudoscalar states π^0 and η). The potential can, in principle, be computed by non-perturbative QCD, such as lattice methods, although this is no easy task. We can, however estimate it in a simple way by considering the second derivative of the effective potential at its minimum,

$$m_a^2 = \left\langle \frac{\partial^2 V_{\mathrm{eff}}}{\partial a^2} \right\rangle \Bigg|_{\langle a \rangle} \propto \frac{1}{f_a^2}.$$

Estimates of standard axion mass have been derived using several methods such as current algebra [53] and effective Lagrangian [30, 54] approaches. Results are

model-dependent, but m_a was widely expected to lie in the 100 keV to 1 MeV region.

Quite generally, Goldstone bosons only have derivative-coupled interactions.[18] However, the axion is a pseudo-Goldstone boson, and the anomalous behaviour of the PQ current generates non-derivative couplings to photons and gluons through the triangle anomaly (see Figure 4.1). This anomalous coupling is, of course, what explicitly breaks the PQ symmetry. The fact that the axion couples to photons means that there is an axion decay channel $a \to \gamma\gamma$, which is important for hopes of detection, to which we shall return in the following section. The interaction Lagrangian is [50, 30]:

$$\mathscr{L}_{a\gamma\gamma} = -\frac{g_{a\gamma\gamma}}{4} F_{\mu\nu}\widetilde{F}^{\mu\nu} a$$

where F is the usual EM field strength and $\widetilde{F}$ is the dual. The coupling constant g can be written

$$g_{a\gamma\gamma} = \frac{\alpha}{2\pi}\left(\frac{E}{N} - \frac{2}{3}\frac{4+z}{1+z}\right)\frac{1+z}{z^{1/2}}\frac{m_a}{m_\pi f_\pi} \tag{4.8}$$

where z is the ratio of the u and d masses and E, N are model-dependent parameters[19]. The standard axion also has derivate couplings to fermions i:

$$\mathscr{L}_{aii} = \frac{g_{aii}}{2m_i}\bar{\Psi}_i\gamma^\mu\gamma^5\Psi_i\partial_\mu a.$$

The PQWW model assigns the same PQ charge to quarks of the same chirality. We can write the Yukawa interactions between quarks (for simplicity—a lepton extension is straightforward) and Higgs fields

$$\mathscr{L}^{\text{PQWW}}_{\text{Yukawa}} = \Gamma^u_{ij}\bar{Q}_{Li}\Phi_1 u_{Rj} + \Gamma^d_{ij}\bar{Q}_{Li}\Phi_2 d_{Rj} + \text{h.c.}$$

where Q_L are left-handed doublets; u_R, d_R are right-handed singlets; $\Phi_{1,2}$ are the Higgs doublets and i, j are family indices. From this structure, it is clear that Φ_1 only couples to right-handed u-type quarks and Φ_2 only to right-handed d-type quarks. This ensures that the theory contains no Higgs-mediated flavour-changing neutral currents (FCNCs) [54].

Alongside this standard axion model, *variant axion* models were also developed, which also assume $f_a \approx v_F$, but now instead allowing axion-quark couplings which differ even for quarks of the same type.[20] This fact introduces

[18] That is to say, only total derivatives of the Goldstone boson fields appear in interaction terms. This is because the Goldstone fields translate under the associated broken symmetries.

[19] E and N represent the QED and QCD anomalies associated with the axial current, respectively. E/N is taken as 8/3 in DFSZ models and 0 in the KSVZ scheme. See below.

[20] These models were originally constructed in order to save the standard axion by tweaking the individual quark couplings, so that the axion was no longer ruled out by contemporary laboratory limits.

(unwanted) Higgs-driven FCNCs, but these can be conveniently confined to, for instance, the charm sector [54]. Considering the Yukawa interaction Lagrangian, we write instead

$$\mathscr{L}_{\text{Yukawa}}^{\text{variant}} = \Gamma_{ij}^{u} \bar{Q}_{Li} \Phi_j u_{Rj} + \Gamma_{ij}^{d} \bar{Q}_{Li} \Phi_2 d_{Rj} + \text{h.c.}$$

where variant models now differ in which of the Φ_j's couples to u_{Rj}.

In summary: The standard axion, in its different forms, is ruled out. We will discuss this further in the next section. We have seen that axion mass and couplings depend inversely on the scale of symmetry breaking, the decay constant f_a. This means that, if f_a is very large, as is currently believed, any physical axions must be very light and very weakly coupled. Let us briefly examine the possible properties of such invisible axions.

Invisible axions The first class of invisible axion models we will discuss is the *KSVZ-class*, where the model of Kim [51] and Shifman-Vainshtein-Zakharov [52] is the progenitor. A new complex scalar σ is introduced, along with a new, superheavy quark Q. The scalar and superheavy quark are both singlets under $SU(2)_L \times U(1)_Y$—they have no electroweak interactions.[21] These two new fields are the only carriers of PQ charge. The scalar field has a VEV $\langle\sigma\rangle = \sigma_0$, which is taken to be arbitrarily large. This means that the new quark mass is also large, and, as such, Q becomes experimentally invisible and the axion becomes arbitrarily light. As before, the axion field enters as the phase of the scalar field σ. From the above, it follows that the axion does not have tree-level interactions with the SM quarks. Such a coupling can, however, happen through, for instance, Q loops. Similarly to the standard axion, 't Hooft instantons generate couplings to gluons and photons. In the original paper by Shifman, Vainshtein and Zakharov [52], an expression for the axion mass is derived:

$$m_a = \frac{f_\pi m_\pi}{4\sigma_0} \left[\frac{4 m_u m_d}{(m_u + m_d)^2}\right]^{1/2} [1 + \mathcal{O}(m_{u,d}/m_s)].$$

Here, m_π and f_π are the pion mass and decay constant. Kim arrives at an (admittedly crude) numerical estimate of $m_a \lesssim 10^{-3}$ eV. [51].

Models such as those due to Zhitnitsky [55] and Dine-Fischler-Srednicki [56] (*DFSZ models*) add to the PQ model just one complex scalar, ϕ, which has no electroweak interactions but does carry PQ charge. There are, as before, two doublets, ϕ_u and ϕ_d, which couple to right-handed up-type and right-handed down-type quarks respectively. The fields acquire nonzero VEVs, which spontaneously breaks the electroweak and PQ symmetries, just like before. The

[21] However, Q is not required to have any specific colour content or charge; they are simply assumed to be the same as for the SM quarks, and 0, respectively. It should be noted that if the charge of Q is 0, there will be stable hadrons with fractional EM charge.

Goldstone boson of the PQ symmetry, which gains a small mass from QCD instantons, is the axion. The DFSZ scheme does not give rise to FCNCs. As for the PQWW axion model, the SM leptons and quarks carry PQ charge. However, we take $\langle\phi\rangle = \frac{1}{\sqrt{2}} f_\phi$ large. The axion decay constant depends on this VEV, and thus the DFSZ axion-matter interactions are, relative to the standard axion model, heavily suppressed. Using a limit $m_a \lesssim 10^{-2}$ eV, the scale is $\langle\phi\rangle > 10^9$ GeV. Extremely large VEVs like this are in the domain of grand unification, and DFSZ axion models are indeed completely compatible with Grand Unified Theories [56].

4.3 Axion status

Ever since the axion was first theorised in the 1970s, a large variety of methods have been used to attempt to find axions or constrain their properties. In addition, some earlier searches for light bosons are also relevant. In this section, we will review the main categories of experiment, citing the most important results, divided into laboratory and astrophysical searches. So far, no axion signal has been observed. A compilation of excluded mass ranges is shown in Figure 4.7.

4.3.1 Axion laboratory searches

As mentioned in the previous section, electroweak-scale PQWW axions were ruled out by laboratory limits shortly after their conception. Due to mixing of the axion state with the light pseudoscalars π^0 and η, the decay of a kaon into a pion and an axion, $K^+ \to \pi^+ a$, must have a nonzero branching ratio. In fact, a theoretical lower limit on this branching ratio can be found. Using PCAC (*Partial Conservation of Axial Current*) and static quark model methods in parallel, T. Goldman and C. M. Hoffman (1978) [57] derive the parameter-independent bounds

$$\mathrm{BR}(K^+ \to \pi^+ a) \gtrsim 4.8 \cdot 10^{-8}$$

and

$$\mathrm{BR}(K^+ \to \pi^+ a) \approx 1.9 \cdot 10^{-8}$$

for each method respectively. Further considerations provide even better limits: J.-M. Frère, et al. (1981) [58] (refining the estimate of Wise (1981) [59]) obtain

$$\mathrm{BR}(K^+ \to \pi^+ a) \approx 0.8 \cdot 10^{-6}.$$

The E949 experiment at BNL [103], among others, has measured $\mathrm{BR}(K^+ \to \pi^+ X^0)$, where X^0 is a new, light particle (like the axion). The 90% CL limit is

$$\mathrm{BR}(K^+ \to \pi^+ X^0) < 0.7 \cdot 10^{-10}.$$

Clearly, these results are in stark disagreement with the theoretical predictions. When we also take into account theoretical bounds from the process $\Upsilon \to a\gamma$ [54], which offer further non-satisfied constraints, the standard axion is to be

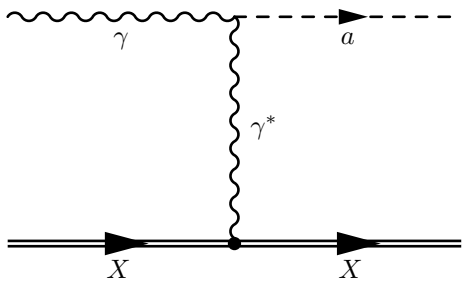

Figure 4.5: *The Primakoff process, in which an axion a is resonantly produced by the triangle anomaly-coupling to two photons. X is a charged particle, which emits a virtual photon.*

considered disproven.

Let us now turn to the still-viable invisible axions. Though the most important (and remarkable) limits on invisible axions come from cosmology and stellar astronomy, as we shall see in the next section, laboratory searches are an important complement, and several have been undertaken. Most such searches rely on the fact that axions, as we have seen, couple to two photons by the Adler-Bell-Jackiw anomaly. This coupling facilitates the production of axions via $\gamma\gamma \to a$ and a corresponding decay channel $a \to \gamma\gamma$. In the presence of an external EM field, the scattering process $\gamma X \to Xa$, where X is some heavy charged particle (e.g. an atomic nucleus), can occur. This is called the Primakoff process [66]. A diagram is shown in Figure 4.5. This phenomenon is sometimes also described as an axion-photon oscillation. One large class of invisible axion searches is based on *photon regeneration*, or "shining light through a wall", LSW. One popular setup [60] is to fire a laser beam along a strong dipole magnet. A small number of axions (or indeed any light, neutral pseudoscalar), if they exist, are produced by the Primakoff process. An obstacle is placed in the beamline, which absorbs all photons, while any axions produced are transmitted. On the other side of the barrier, there is another magnet. In the presence of this field, the axions in the beam may reconvert into photons, which are subsequently detected. Both the conversion probabilities and the momenta of regenerated photons are straightforward to predict [60].

Recently, this setup was used in the experiment performed by the ALPS Collaboration [61], using a dipole magnet from the HERA ring at DESY as outlined above. The setup is shown schematically in Figure 4.6. The result was a limit on the conversion probability, to 95% CL, of

$$P(\gamma \leftrightarrow a) \lesssim 10^{-25}.$$

We might, in a different setup, detect axion conversion directly from changes in the polarisation of a photon beam propagating through a magnetic field [62]. Photons which are polarised parallel to the field mix with the axion state, while

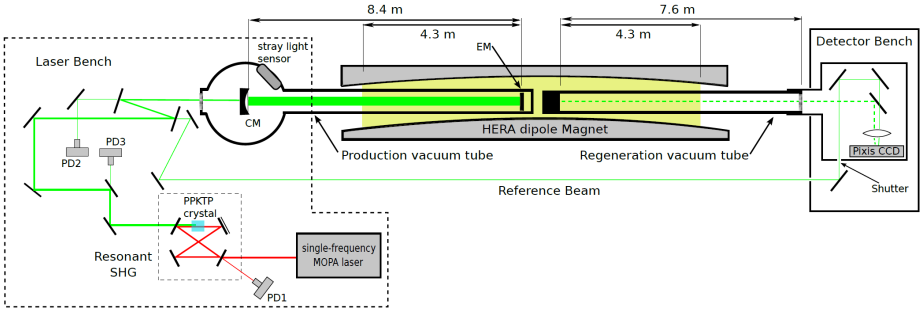

Figure 4.6: *Experimental setup of the ALPS LSW experiment [61]. A photon beam is generated in the laser branch (left), and made to pass through a strong magnetic field, generated by a HERA dipole magnet (centre). An obstacle halfway down the magnet blocks all photons, but any axions, produced by the Primakoff process, will pass through. Some axions will regenerate into photons in the remainder of the flight, and any such photons are detected by a CCD sensor in the detector branch (right).*

orthogonal polarisations do not, and thus a rotation of the polarisation of the beam may be detected. This rotation depends on the axion mass, and vanishes as m_a becomes large. For this reason, the known physical pseudoscalars, π^0 and η, which are heavy in the context, produce no effect. This setup also gives a handle on the photonic coupling of any observed axion, in addition to the mass.

The PVLAS collaboration used this type of experiment to detect a signal possibly ascribable to a light pseudoscalar [64]. However, this interpretation was later excluded when improved limits were obtained by the same group [65].

4.3.2 Astrophysical limits

The most important modern limits on axion interactions and masses are found in astrophysics. We will focus on two main classes of research: limits derived from energy loss in stars, due to axion production and their subsequent escape, and direct axion flux searches. We will first discuss limits on axion couplings and mass derived from stellar astronomy and on observation of the supernova event SN 1987A. Finally, we review attempts to directly detect axions from astronomical sources.

Energy-loss limits Axions, should they exist, are produced to a great extent inside stars. This takes place primarily by the Primakoff process, as shown in Figure 4.5, in the strong EM fields in the bulk of the star. Since axions are weakly interacting, they pass through the star and be emitted in very large numbers. This means energy escapes. There are sophisticated and experimentally successful models of stellar evolution (such as the Standard Solar Model). Since

the evolution of mass, luminosity and other properties is precisely predicted, and dependent on escaping mass, upper bounds can be acquired on such energy loss by fitting the models to observation. We will now outline how a limit on the axion-photon coupling $g_{a\gamma\gamma}$ can be obtained using this method.

First, we need an expression for the axion flux. Such a calculation is far outside the scope of our review, so we will simply quote the result: once the solar volume has been integrated over, using a modern solar model, the solar axion luminosity is given by [67]

$$L_a = g_{10}^2 1.85 \cdot 10^{-3} L_\odot.$$

Here, $g_{10} = g_{a\gamma\gamma} 10^{-10}$ GeV and $L_\odot$ is the solar photon luminosity.

Now, $L_\odot$ is of course fixed. Axion energy losses would lead to an increased rate of nuclear fuel consumption [68], which in turn means an increased neutrino flux. This all-flavour flux has been measured by the SNO Collaboration [69]. Using these results, in conjunction with the above flux yields [70] $L_a \lesssim 0.04 L_\odot$, which implies

$$g_{a\gamma\gamma} \lesssim 5 \cdot 10^{-10} \text{ GeV}^{-1}.$$

Globular clusters (GCs) are dense, spherical collections of stars, usually containing $10^5 - 10^6$ stars. They are useful objects of study: Since all the contained stars are formed at roughly the same time, they mainly differ in mass. This means that globular clusters provide large, homogeneous populations of stars, well-suited to tests of models of stellar formation and evolution. Axion coupling limits can be found from GCs by first computing the change in the predicted lifetime of *horizontal branch* (HB) stars[22]. To good approximation, an expression for the energy loss rate per unit volume due to the Primakoff process in a star is [68]

$$Q = \frac{g_{a\gamma\gamma}^2 T^7}{4\pi} F$$

where F is a constant of order 1 and T is the temperature. Using this, and averaging over a typical HB star core, we can find the increased rate of core helium consumption and the resulting reduction in lifetime. For $g_{a\gamma\gamma} = 10^{-10}$ GeV^{-1}, this is about 30% [68]. Now, red giants are much less affected by axion energy loss. Comparison of the number of HB stars with the number of red giants (and thus the ratio of the lifetimes of the two phases) in a given cluster shows agreement of the helium burn rate with expectations on the 10% level [71]. From this, we can state a conservative limit of

$$g_{a\gamma\gamma} < 10^{-10} \text{ GeV}^{-1},$$

which, of course, is more restrictive than the solar limits discussed above.

Assuming the coupling strength limit above, we can find mass limits via Equation (4.8). Using, in line with the literature, $z = m_u/m_d = 0.56$, we obtain

[22] These are stars that lie in the so-called horizontal branch region of a colour-magnitude diagram. These stars burn helium in their core and hydrogen in a shell surrounding it.

for KSVZ-type axions ($E/N = 0$)

$$m_a < 0.3 \text{ eV}$$

and for DFSZ models ($E/N = 8/3$)

$$m_a < 0.7 \text{ eV}.$$

The event known as SN 1987A was a supernova in the Large Magellanic Cloud, whose light was observed on Earth in February 1987. At a distance of 160,000 ly, it was the closest supernova to Earth since the advent of modern astronomy. Apart from offering unprecedented observations for stellar astronomy, a burst of neutrinos was also detected, lasting about ten seconds[23], allowing several new bounds to be placed on neutrino mass, charge and other properties. Limits on axion couplings can be based on the duration of this neutrino signal, as we shall see. In the supernova, the core of the collapsed star forms a proto-neutron star, an object so massive and hot that even even neutrinos are severely slowed. During the phase of neutrino emission, energy can be more efficiently carried away by axions, thus depriving the neutrino cooling channel of energy. This would imply a decrease in the neutrino burst duration.

Axions would be emitted by nucleon bremsstrahlung, $N + N \to N + N + a$. The neutrino signal constrains the coupling g_{aNN} of axions to the nucleonic matter inside the core. A necessarily rough calculation for hadronic axions [68] yields

$$f_a \gtrsim 4 \cdot 10^8 \text{ GeV},$$

corresponding to

$$m_a \lesssim 16 \text{ meV}.$$

If the coupling is too strong, the axions will become trapped as well, leaving the neutrino burst duration unaffected. Thus, only around three orders of magnitude can be excluded. For even stronger couplings, however, axions would (despite the very low number emitted) produce extra, unobserved events in the neutrino detectors. Thus, the excluded range is significantly increased.

If the axion-photon coupling is smaller than assumed, there might exist a window of approximately one order of magnitude, the *hadronic axion window*, between the excluded regions [86]. However, this window is now closed by dark matter limits, as we shall see in the next chapter.

Finally, we will note that similar energy loss arguments can be used in a number of further situations. One example is the cooling of white dwarf stars via axion escape, which affects the period of pulsating white dwarves. This constrains axion-electron coupling in analogy with the reasoning put forward above.

[23] In fact, the three main neutrino observatories in the world (Kamioka, IMB and BNO) registered only 24 counts in total.

Direct searches Solar axions can be detected by *axion helioscopes*, by essentially pointing a large magnet at the sun: Any incident axions will thus pass through a strong EM field, and the resulting photon recombination can be measured (in analogy to the laboratory LSW experiments discussed in Section 4.3.1). Here, we will cover some of the results of the CERN Axion Solar Telescope (CAST) [72], the current, leading axion helioscope.

CAST uses a 9 m long LHC prototype magnet, with $B = 9$ T, in conjunction with solid state x-ray detectors. The setup is mounted on a turning platform so that it can track the Sun. If solar axions are emitted, additional photon counts will be expected when the magnet is aligned with the Sun. The conversion volume is filled with He, acting as a buffer gas, producing a virtual photon mass and thus increasing the probability of reconversion.

The non-observation of events has constrained the product $g_{aee}g_{a\gamma\gamma}$ for non-hadronic axions. The axion-photon coupling enters through the recombination process which produces a signal in the helioscope. Non-hadronic axions, which couple directly to leptons, are expected to be produced in the Sun primarily through *BCA* reactions: bremsstrahlung ($e+e \to e+e+a$), Compton scattering ($\gamma+e \to \gamma+a$) and *axio-recombination* ($e+I \to I^- + a$). This is in turn expected to produce higher solar fluxes than for hadronic axions.

To 95% CL, the CAST experiment [73] has found, for axions with $m_a \leq 10$ meV,

$$g_{aee}g_{a\gamma\gamma} \lesssim 8.1 \cdot 10^{-23} \text{ GeV}^{-1}$$

For hadronic axions, the primary production method is the Primakoff process. Recent CAST runs [74] have constrained the axion-photon coupling in the mass range $0.39 \text{ eV} \lesssim m_a \lesssim 0.64$ eV. They found, to 95% CL,

$$g_{a\gamma\gamma} \lesssim 2.3 \cdot 10^{-10} \text{ GeV}^{-1}.$$

Very recently, axion-photon coupling limits have been found from gamma ray observations by the Cherenkov telescope array H.E.S.S. (High Energy Stereoscopic System) [102]. These mark the first exclusions from gamma ray astronomy. Axion-photon oscillations would alter the opacity of the Universe to high-energy photons. The TeV photon emitter PKS 2155-304 was studied, using estimates on the B field strength in its vicinity, allowing comparison of the predicted spectral shape for some sample axion-like particle models to measurements. H.E.S.S. is currently only sensitive to very light axions, $10 \text{ neV} < m_a < 100$ neV, but within this mass range competitive constraints can be placed on $g_{a\gamma\gamma}$, improving on CAST limits for a part of the mentioned mass range. We refer to [102] for the excluded regions.

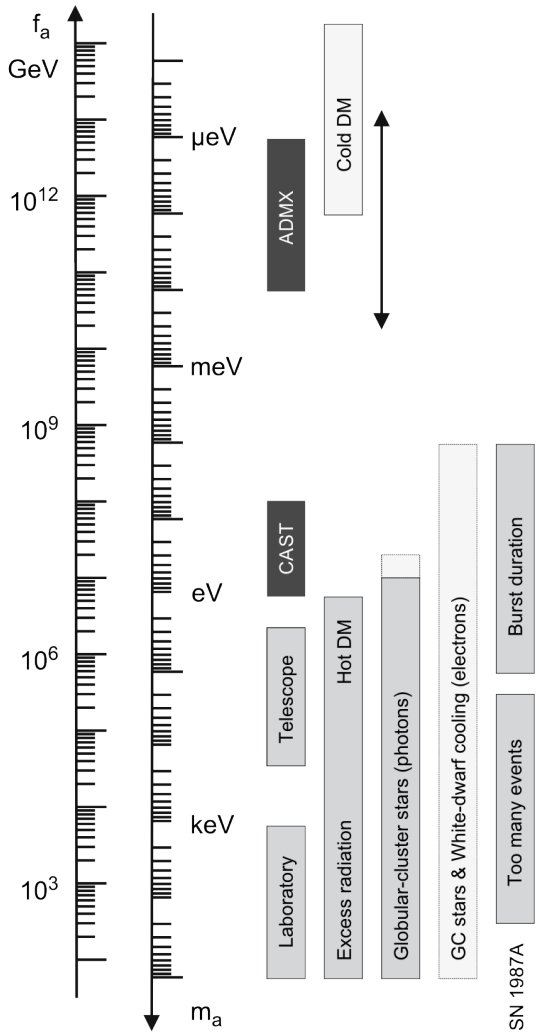

Figure 4.7: *Regions excluded by various experiments [68]. Light-grey fields strongly depend on model. The limits from DM observations and the ADMX experiment are discussed in Chapter 5.*

5 Axion cosmology and dark matter

5.1 Dark matter

Dark matter (DM) is the name given to the 'missing mass' in the Universe which was first inferred by studying the orbital velocities of galaxies in clusters, in the 1930s. We will now give a short overview of DM, and detail the main popular candidate particles for dark matter, reviewing the axion in this context in the following section.

The DM hypothesis has been supported by a wide range of observations, mainly of large-scale structures[24], and more recently analysis of the power spectrum of the cosmic microwave background[25]. According to the 2013 Planck data release [75], DM contributes around 27% of the energy content of the Universe (while ordinary matter only comprises 5%). DM is usually assumed to consist of one or several new species of weakly interacting particles. It must, to very close approximation, be electrically uncharged (or it would not be dark) and gravitationally interacting. Interactions under the weak and strong forces are generally allowed, depending on model. DM cannot consist to any large degree of baryonic matter, as the baryon density in the Universe is tightly constrained by, among other things, CMBR measurements [75].

DM is usually subdivided into three types: *cold*, *hot* and *warm*. This pertains to objects or particles that have small, large and intermediate *free-streaming lengths*, respectively. This length is the possible distance of travel due to random velocities in the early Universe, adjusted for the expansion of the Universe—a characteristic length scale. Since the particles can propagate freely over this distance scale, any smaller fine-scale structure is smoothed out.

Cold dark matter If a DM particle's mass is much greater than the temperature at which it decouples[26] from the cosmological plasma, $m \gtrsim T_d$, it is called Cold DM (CDM). These particles are then nonrelativistic at the point of decoupling, and have a short *free-streaming length*, $\lesssim 1$ Mpc. CDM particles become nonrelativistic early in time after the Big Bang, and are massive and slow in the context.

The assumption of the existence of CDM, as part of the standard cosmological ΛCDM model, predicts the large-scale structure of the Universe well. However, CDM's small free-streaming scale means that there should be an abundance of (small-scale) satellite galaxies in the Universe, contrary to observation. This is known as the *missing satellites problem*. A potential solution to this problem is that some of the missing galaxies simply have a much lower

[24] DM can be inferred from, among other things, the velocity dispersion of galaxies and gravitational lensing.

[25] The power spectrum plotted as a function of angular scale displays a series of peaks. The characteristics of the third peak are sensitive to the dark matter-radiation ratio of the Universe.

[26] That is, essentially, stops interacting. This occurs as the rate of interaction becomes comparable to the rate of cosmological expansion.

mass-to-light ratio than expected, rendering them effectively invisible. In fact, new discoveries of ultra-feint satellite galaxies have significantly alleviated the discrepancy [76].

In the CDM paradigm, large-scale structure is formed *bottom-up*, with smaller structures being formed first and then merging.

We will now give a short list of the main CDM candidates.

- *WIMPs, Weakly Interacting Massive Particles*, is a class of heavy hypothetical particles, and one of the leading CDM prospects. They do not interact strongly or electromagnetically, but weakly, and possibly by other new fundamental forces. Any such new interactions must, however, occur at low cross-sections. Their large mass (typically 10–1000 GeV) means they are considered cold.

  In the early, hot Universe, any DM particle would be copiously pair-produced, until the Universe cools below some critical temperature. Meanwhile, the particles pairwise annihilate. The rate of annihilation tapers off as the Universe expands and the particle density decreases. The remaining density at the present time is called the *relic density*. The predicted annhihilation cross-section required to reproduce the current DM density fits weak interactions very well, which is one reason WIMPs are popular candidates. This sometimes called the *WIMP "miracle"*.

  WIMP DM candidates notably come from SUSY: In the Minimally Supersymmetric Standard Model extension, where R-parity[27] conservation is imposed, the necessarily stable lightest neutralino[28] would be a promising candidate.

- CDM Axions. See Section 5.2.

- *MACHOs, MAssive Compact Halo Objects*. These are not particles, but astronomical bodies such as black holes, planets, neutron stars or faint red and white dwarf stars. Due to the aforementioned limits on baryonic matter, and unsuccessful direct searches for the microlensing caused by such objects [77], among other things, MACHOs are generally considered to be ruled out of explaining most of the missing mass.

- Gravitinos, the supersymmetric partners of gravitons. If they are thermally produced, stable LSPs with masses $\gtrsim 100$ keV, they could comprise CDM [79].

Hot dark matter Hot DM (HDM) consists of particles with masses satisfying $m \lesssim T_d$, which means that they are still relativisitic by the time of their decoupling. In addition, HDM is defined as particles with $m \lesssim 1$ eV, which is

[27] Recall that R-parity is defined as $P_R = (-1)^{2S+3B+L}$, where S, B and L are spin, baryon number and lepton number, respectively. All SM particles have $P_R = 1$ and all SUSY partners have $P_R = -1$.

[28] The neutralino is a Majorana linear combination of neutral gaugeino and Higgsino states.

the temperature at which the Universe energy density moves from being radiation dominated to matter dominated. HDM particles have long free-streaming lengths, $\gtrsim$ 1 Mpc. Their free-streaming scale is much larger than the protogalactic scale. Thus, structure formation occurs in a top-down manner: Large structures are formed first, as any structure of galactic scale or smaller would be smeared out. These would subsequently be broken down into smaller fragments. However, this stands in contradiction to modern deep-field astronomy, from which it may clearly be seen that small-scale structures like galaxies were formed earlier than can be explained by this type of model. As such, HDM is no longer generally considered able to make up more than a small fraction of the total DM density.

A couple of example candidates are:

- Neutrinos, the archetypal HDM particle. However, since they are known to be extremely abundant in the Universe, they must be very light in order for the structures they form not to suffer gravitational collapse. (Neutrino masses are, of course, also constrained by other sources.) Their required lightness makes them hot, and thus neutrino-based DM fails to explain the small-scale structure of the Universe.
- HDM Axions. See Section 5.2.

Warm dark matter Warm DM (WDM) lies, as the name implies, between HDM and CDM. As for HDM, WDM has $m \lesssim T_d$, but now $m \gtrsim 1$ eV, so WDM particles were relativistic at their decoupling temperature, but nonrelativistic at the time of matter-radiation equality. The free-streaming size is of dwarf-galaxy scale, or ~ 1 Mpc. Structure formation in this paradigm occurs top-down (bottom-up) on scales smaller (larger) than the free-streaming scale. WDM models share the successful large-scale explanatory power of CDM, and several simulations [78] indicate that WDM is better suited to explaining the small-scale structure of the Universe.

There are no clear candidates for WDM. Below, we list some propositions.

- Non-thermally produced WIMPs. These WIMPS could have a considerably longer free-streaming length than CDM WIMPs, which would allow them to serve as WDM particles.
- Gravitinos. If non-thermally produced, e.g. through the decay of a (heavier and charged) slepton NLSP (Next-to-Lightest Supersymmetric Particle), gravitinos could be viable as a WDM candidate [79]. The NLSPs could be produced in the early Universe, later decaying into gravitinos. Produced at high momenta, they would smoothen out fine-scale structure.
- *Sterile neutrinos* are undiscovered, heavy fermions which are singlets under all SM gauge groups. They are commonly introduced to explain the smallness of the SM neutrino masses.[29] These are especially interesting if

[29] The *see-saw mechanism* generates small masses for the observed neutrinos by postulating heavy, undiscovered neutrinos.

they have a mass of ~ 1 keV, in which case they would participate in other effects, such as star formation [80] (though, it should be noted, the see-saw mechanism works best for sterile neutrinos much heavier than this). Due to mixing with the SM neutrinos, the rate of decay to a lighter neutrino and a photon would be small but nonzero. Non-observation of such a photon signal casts some doubt on sterile neutrinos as DM candidates [81].

5.2 The axion as a dark matter candidate

The axion is considered a promising and well-motivated candidate for dark matter. Depending on the production process (thermal or non-thermal), axions could constitute both warm and cold dark matter. We consider HDM axions in Section 5.2.1. CDM axions are usually considered more viable, and are treated in Section 5.2.2. Finally, we will review searches and the current status of axion DM in Section 5.3.

5.2.1 HDM axions

Axions would be produced thermally in the early Universe. Hadronic axions (which do not couple directly to charged leptons) would be produced by Primakoff reactions (Fig. 4.5) with the quarks in the primordial quark-gluon plasma (QGP) [82]. After the temperature of the Universe drops below Λ_{QCD} and confinement occurs, the dominant thermalisation process is $\pi + \pi \leftrightarrow a + \pi$ [84].

5.2.2 CDM axions

Since HDM, no matter what the constituents are, seemingly cannot make up more than a small part of the total DM density, axionic CDM is usually more seriously considered. Cold axions are produced by two processes; vacuum realignment in the so-called *misalignment mechanism* [89, 90, 91] and the decay of topological strings and walls [94]. Dealing with this topic fully is beyond the scope of this text, but we shall attempt a basic summary.

There are two important phase transitions to consider when discussing cold axion production. The first is the spontaneous breaking of the $U_{\mathrm{PQ}}(1)$ symmetry, at $T = f_a = T_{\mathrm{PQ}}$. The second is the QCD phase transition, at $T = T_{\mathrm{QCD}} \approx 1$ GeV, where QCD effects become important [92].

Early in the Universe, at very high T, the axion potential is described by Figure 3.1a. As $T = T_{\mathrm{PQ}}$, the PQ symmetry is spontaneously broken, and the potential takes some random value along the circle of potential minimum, shown in Figure 3.1b. The assumed value is different in causally disconnected regions of spacetime.

Meanwhile, at $T = T_{\mathrm{QCD}}$, QCD effects kick in and the potential is tilted by the instantons described in Section 4; the PQ symmetry is explicitly broken

and the axion becomes massive. This is, of course, the PQ mechanism. When this explicit breaking occurs, the axion field will begin oscillating, rolling in its potential. These oscillations constitute nonrelativistic particles, contributing to a CDM population. The production of cold axions in this way is called the *misalignment mechanism*, and it is discussed further below. Cold axions are produced in this way regardless of additional topological production.

Now, there are two possible scenarios for us to consider. These depend on whether the inflationary *reheat temperature*[30] T_R is higher or lower than T_{PQ}. If $T_R < T_{\mathrm{PQ}}$, the axion field will be homogenised over very large scales [93], and no topological defects will be formed in the field. However, if $T_R > T_{\mathrm{PQ}}$, *cosmic strings* and *domain walls* will be formed. The decays of these radiate axions. This is the topological production process of cold axions, discussed below.

Misalignment mechanism The PQ mechanism lets the vacuum angle θ go to 0 naturally by promoting it, as we have seen, to a dynamical field and letting it relax to a potential minimum. In fact, this evolution to the minimum occurs by means of a dampened oscillation [93]. This occurs once QCD effects become important and the axion field begins to feel its mass. At some critical temperature T_1, at time t_1, defined as $m_a t_1 \sim 1$, the axion field begins to oscillate around the potential minimum. Note that the mass depends on the potential (recall Section 4.2.1), and thus on temperature and time. This occurs as $T \approx 1$ GeV.

In the case where $T_R < T_{\mathrm{PQ}}$, the oscillation is comprised of one zero-momentum mode. When the axion field rolls in its potential, it constitutes a coherent condensate of particles at rest.

In the second case, where $T_R > T_{\mathrm{PQ}}$, the axion field varies with both time and space, since it has not been homogenised by inflation. There are now, in addition to the zero-momentum mode in the former case, nonzero modes of oscillation. Although, in this case too, the velocity dispersion of the particles can be shown to be very small [95].

At late times, the (comoving) axion number density remains constant. The current energy density may then be extrapolated from estimates of early number densities [95].

Topological decay If $T_R > T_{\mathrm{PQ}}$, and the spontaneous breaking of the PQ symmetry occurs after inflation, different regions of space will possess different vacuum angles. So-called strings and domain walls appear, which are 1- and 2-dimensional topological defects, arising from the fact that the axion field cannot homogenise past causal horizons. These annihilate due to tension and radiate cold axions in doing so. As a technical discussion is beyond the scope of an undergradute level text, we will not enter into one. There is some controversy regarding the size of the contribution: Sikivie [95] estimates production from

[30] When inflation occurs, T is drastically lowered as space expands. When inflation slows, the temperature rises again. This is reheating.

wall decay to be subdominant to that from string decay and vacuum alignment. Other authors [97] find the string and wall decay contributions much larger.

Combining these production methods, expressions for the axion energy density at the present epoch can be derived. According to P. Sikivie [95], in the case of $T_R < T_{\rm PQ}$, where the PQ symmetry is broken before inflation halts,

$$\Omega_a \sim 0.15 \left(\frac{f_a}{10^{12}\ \text{GeV}} \right)^{7/6} \left(\frac{0.7}{h} \right)^2 \theta_i^2.$$

Here, θ_i is the initial random value of the vacuum angle, the *misalignment angle*, and h is the reduced Hubble parameter, $h = H_0/(100\ \text{km}/(\text{s} \cdot \text{Mpc}))$.

In the case where $T_R > T_{\rm PQ}$, inflation occurs before the breaking of the PQ symmetry. Here, we have topological production in addition to the misalignment mechanism. Averaging over the misalignment angles assumed in the different domains, and neglecting wall decay production, we have

$$\Omega_a \sim 0.7 \left(\frac{f_a}{10^{12}\ \text{GeV}} \right)^{7/6} \left(\frac{0.7}{h} \right)^2 .$$

Comparing this to the measured CDM density provides an approximate lower limit of $m_a \sim 10\ \mu$eV.

If the PQ phase transition happens after inflation, the axion field will be inhomogeneous, and causally disconnected regions will have different misalignment angles. The free-streaming lengths of the produced axions [95] are not large enough to smoothen these inhomogeneities, which leads to the formation of *axion miniclusters*. These are gravitationally bound objects with masses $\sim 10^{-12} M_\odot$ and radii $\sim 10^{10}$ cm, which are in theory detectable by gravitational lensing [98].

5.3 Axion DM searches and status

Here, we will detail searches for and limits on DM axions. We will first review telescope HDM searches. In Section 5.3.2 we will discuss the ADMX microwave cavity experiment, which is currently the best hope for detecting or realistically excluding CDM axions.

5.3.1 HDM axion status

First, let us consider HDM axions. A thermal axion population would contribute to HDM, and cosmological limits on such DM components (discussed in Section 5.1) yield axion mass constraints: For hadronic axions, a recent limit using Planck and Hubble satellite data [85] is

$$m_a < 0.67\ \text{eV} \text{ or } f_a > 5.7 \cdot 10^6\ \text{GeV},$$

notably similar to neutrino mass limits derived from the same arguments. This result thus closes the 'hadronic axion window' left open by the SN 1987A data and other astrophysical observations (see Section 4.3.2).

After the QCD epoch, axions decouple if $m_a \gtrsim 0.2$ eV [68]. Some of the relic axions would be trapped in galaxy clusters and, due to their large number, some would decay via $a \to \gamma\gamma$. This would produce an optical decay line corresponding to the axion mass. Telescope searches have been unsuccessful, providing axion mass limits. See the 'Telescope' field in Figure 4.7 and, for example, [87].

If $m_a \gtrsim 20$ eV, axions will decay rapidly compared to cosmic time scales. This would provide an excess of photons, distorting the CMB spectrum and destroying primordial deuterium [88]. Nonobservation of these effects constrains the abundance of such particles, roughly shown by the 'Excess radiation' field in Figure 4.7.

5.3.2 CDM axion status: the ADMX experiment

There is currently only one experiment which realistically probes CDM axions—the *Axion Dark Matter eXperiment, ADMX* [99]. Running since 1996 at Lawrence Livermore National Laboratory, it is the first experiment to probe realistic regions of axion parameter space. The ADMX setup consists of a microwave cavity, permeated by a strong (8 T) magnetic field and cooled to a temperature of a few K. The cavity can be tuned (that is, the resonance shifted) by moving metal or dielectric rods hung inside the cavity. Axions in the dark matter halo of our galaxy undergo photonic conversion in the presence of the magnetic field. The resulting, extremely weak, microwave signal is seen as a resonance in the chamber when its frequency is tuned to the total axion energy. As the frequency band is scanned and rescanned, any true axion signal will consistently reappear in the same frequency bin, while statistical fluctuations and background signals will not. The setup is depicted schematically in Figure 5.1.

The most recent run [100] excluded, to 90% CL, a new swathe through parameter space. This is displayed in Figure 5.2. This assumes a local DM density of 0.45 GeV/cm^3. *Virialised* (dynamically equilibrated) and *unvirialised* refers to two different models of DM distribution: The 'virialised' case assumes a DM velocity dispersion of 160 km/s, and a speed of the halo relative to earth of 220 km/s. The 'unvirialised' scenario has a velocity dispersion and a relative speed of less than 60 km/s. The yellow band represents the region in parameter space occupied by common axion models. As shown, the ADMX experiment excludes realistic axion models: The combined ADMX mass exclusion now ranges between 1.9 μeV and 3.53 μeV.

In addition, upgrades will be made to the ADMX setup [101]. Improved cooling will allow the experiment to run at ~ 100 mK instead of the current ~ 2 K. This will bring significant improvements in search efficiency and range: The experiment will be "sensitive to even the most pessimistic axion-photon

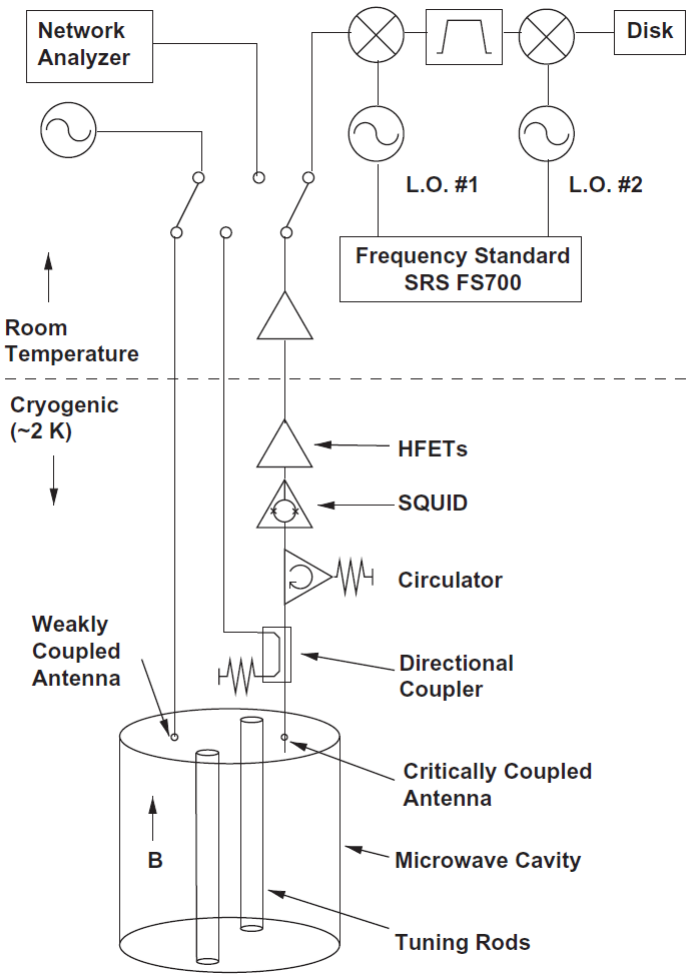

Figure 5.1: *Schematic overview of the ADMX setup [101]. At the bottom is the microwave cavity, 1 m long and 0.5 m in diameter, which contains several metal or dielectric tuning rods. As the rods are moved into different configurations inside the cavity, the resonance frequency is altered. Antennas sample the EM field and the signal is first amplified then shifted to a lower frequency, before it is saved. We will not discuss the signal processing or electronics in any detail; for a full description, please see [101].*

couplings over the entire axion mass range while still scanning ten times as fast as the present detector" [100]. These planned upgrades will allow axion exclusion over the mass range 1–100 μeV, covering two of the three orders of magnitude of the window shown in Figure 4.7, the expected axion CDM range.

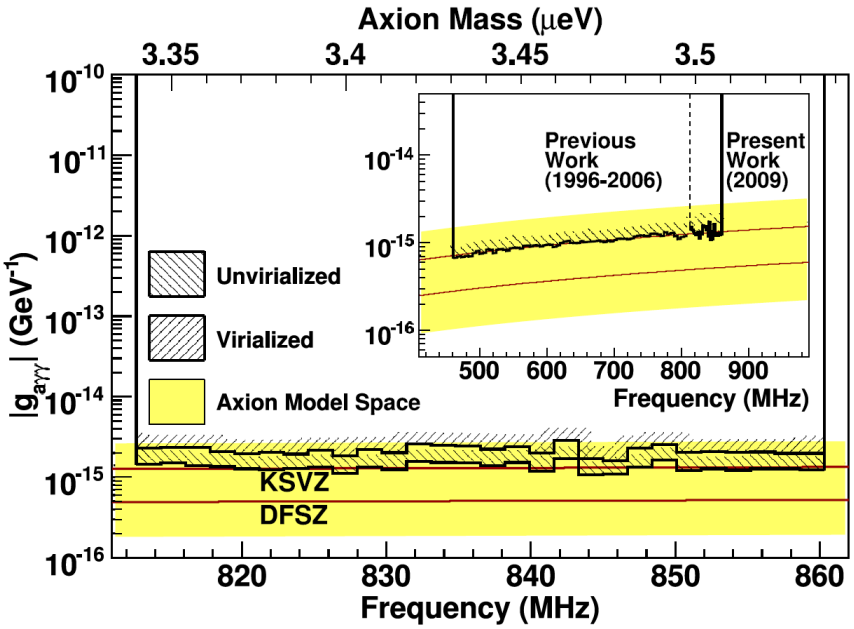

Figure 5.2: *Past and current ADMX exclusion regions in axion parameter $(m_a, g_{a\gamma\gamma})$ space [100], for the virialised and unvirialised scenarios discussed in the text. The frequencies shown are the chamber resonance frequencies corresponding to each axion mass. The approximate parameter regions for KSVZ and DFSZ model classes are shown in yellow.*

Both discovery and exclusion would have a major impact on the viability of CDM axions.

6 Summary, conclusions and outlook

In conclusion, the spontaneous breaking of a new PQ symmetry is a beautiful and powerful solution to the strong CP problem. Axions with μeV to meV masses would be copiously produced in the early universe and fit excellently the role of cold dark matter. This, in addition to the naturalness and parsimony stemming from the strong independent arguments for its existence, makes the axion highly relevant as a DM candidate. Near-future experiments will be able to probe a significant fraction of interesting parameter space.

6.1 Acknowledgments

The author wishes to thank Torsten Åkesson and Johan Rathsman for their time and guidance, and Peter Corrigan for his advice on language.

References

[1] The SNO Collaboration, *Combined Analysis of all Three Phases of Solar Neutrino Data from the Sudbury Neutrino Observatory.* arXiv:1109.0763v1 [nucl-ex], 2011.

[2] G. Kane, *Modern Elementary Particle Physics.* Perseus Publishing, Massachusetts, Updated Edition, 1993.

[3] The ATLAS Collaboration, *Observation of a New Particle in the Search for the Standard Model Higgs Boson with the ATLAS Detector at the LHC.* arXiv:1207.7214v2 [hep-ex], 2012.

[4] The CMS Collaboration, *Observation of a new boson at a mass of 125 GeV with the CMS experiment at the LHC.* arXiv:1207.7235 [hep-ex], 2012.

[5] B. R. Martin, G. Shaw, *Particle Physics.* John Wiley & Sons Ltd, 3rd Edition, 2008.

[6] E. Kh. Akhmedov, *Neutrino physics.* arXiv:hep-ph/0001264v2, 2000.

[7] Alan Kostelecky, *Background information on Lorentz and CPT violation.* URL: `http://www.physics.indiana.edu/~kostelec/faq.html`. Data retrieved 31-12-12.

[8] N. Kanning, *The CPT Theorem.* 2009, URL: `http://www.noch-mehr-davon.de/data/vortr/qft/cpt.pdf`. Data retrieved 31-12-12.

[9] O.W. Greenberg, *CPT Violation Implies Violation of Lorentz Invariance.* arXiv:hep-ph/0201258, 2002.

[10] A. Kostelecky and N. Russell, *Data Tables for Lorentz and CPT Violation.* arXiv:0801.0287 [hep-ph], 2008.

[11] A. Kostelecky, *The Status of CPT.* arXiv:hep-ph/9810365, 1998.

[12] J. Beringer et al. (Particle Data Group), *CP violation in meson decays.* Phys. Rev. D**86**, 010001 (2012) URL: `http://pdg.lbl.gov/2011/reviews/rpp2011-rev-cp-violation.pdf`.

[13] The Belle Collaboration, *Improved Measurements of Direct CP Violation in $B \to K^+\pi^-, K^+\pi^0$ and $\pi^+\pi^0$ Decays.* arXiv:hep-ex/0507045, 2005.

[14] J. Beringer et al. (Particle Data Group), *The CKM Quark-Mixing Matrix.* Phys. Rev. D**86** 010001, 2012, URL: `https://pdg.web.cern.ch/pdg/2012/reviews/rpp2012-rev-ckm-matrix.pdf`.

[15] A. D. Sakharov, *Violation of CP invariance, C asymmetry, and baryon asymmetry of the universe.* Sov. Phys. Usp. 34 (5), pp. 392–393, 1991.

[16] J. Goldstone, *Field Theories with Superconductor Solutions*. Nuovo Cimento 19: pp. 154-164, DIO: 10.1007/BF02812722, 1960.

[17] F. Mandl, G. Shaw, *Quantum Field Theory*. John Wiley & Sons Ltd, 2nd Edition, 2010.

[18] J. Goldstone, A. Salam and S. Weinberg, *Broken Symmetries*. Phys. Rev. **127** pp. 965–970 (1962).

[19] C. P. Burgess, *Goldstone and Pseudo-Goldstone Bosons in Nuclear, Particle and Condensed-Matter Physics*. arXiv:hep-th/9808176, 1998.

[20] K. Nakamura et al. (Particle Data Group) *Review of Particle Physics*. J. Phys. G: Nucl. Part. Phys **37** 075021, 2010, URL: `http://pdg.lbl.gov/2011/reviews/rpp2011-rev-quark-masses.pdf`.

[21] K. Nakamura et al. (Particle Data Group) *Review of Particle Physics*. J. Phys. G: Nucl. Part. Phys **37** 075021, 2010.

[22] M. Gell-Mann, *The Eightfold Way: A Theory of Strong Interaction Symmetry*. TID-12608; CTSL-20, 1961, URL: `http://www.osti.gov/energycitations/product.biblio.jsp?osti_id=4008239`

[23] S. Okubo, *Note on Unitary Symmetry in Strong Interactions*. Prog. Theor. Phys. Vol. 27 No. 5 (1962) pp. 949-966, 1962, URL: `http://ptp.ipap.jp/link?PTP/27/949/`

[24] S. Okubo, *Note on Unitary Symmetry in Strong Interaction. II*. Prog. Theor. Phys. Vol. 28 No. 1 (1962) pp. 24-32, 1962, URL: `http://ptp.ipap.jp/link?PTP/28/24/`

[25] S. Weinberg, *The U(1) problem*. Phys. Rev. D**11**, pp. 3583–3593, 1975.

[26] J. S. Bell, R. Jackiw, *A PCAC puzzle: $\pi^0 \to \gamma\gamma$ in the σ-model*. Nuovo Cim. A**60** (1969) 47–61, 1969.

[27] S. Adler, *Axial-Vector Vertex in Spinor Electrodynamics*. Phys. Rev. **177**, pp. 2426–2438 (1969).

[28] G. t'Hooft, *Symmetry Breaking through Bell-Jackiw Anomalies*. Phys. Rev. Lett. **37**, pp. 8–11 (1976).

[29] G. t'Hooft, *Computation of the quantum effects due to a four-dimensional pseudoparticle*. Phys. Rev. D**14**, pp. 3432–3450 (1976).

[30] R. D. Peccei *The Strong CP Problem and Axions*. arXiv:hep-ph/0607268, 2006.

[31] W. Bardeen, *Anomalous currents in gauge field theories*. Nucl. Phys. B **75**, pp. 246–258, 1974.

[32] S. Vandoren, P. van Nieuwenhuizen, *Lectures on instantons*. arXiv:0802.1862 [hep-th], 2008.

[33] R. J. Crewther, *Effects of topological charge in gauge theories*. Acta Phys. Austriaca **9** (1971) pp. 47–153, 1971.

[34] B. L. Ioffe, *Axial anomaly in quantum electro- and chromodynamics and the structure of the vacuum in quantum chromodynamics*. arXiv:0809.0212 [hep-ph], 2008.

[35] R. Jackiw, C. Rebbi, *Vacuum Periodicity in a Yang-Mills Quantum Theory*. Phys. Rev. Lett. **37**, pp. 172–175 (1976), 1976.

[36] Shahida Dar, *The Neutron EDM in the SM : A Review* [sic]. arXiv:hep-ph/0008248v2, 2000.

[37] V.A. Dzuba, V.V. Flambaum, *Parity violation and electric dipole moments in atoms and molecules*. arXiv:1209.2200 [physics.atom-ph], 2012.

[38] R.J. Crewther, P. Di Vecchia, G. Veneziano and E. Witten, *Chiral estimate of the electric dipole moment of the neutron in Quantum Chromodynamics*. Phys. Lett. B**88**, 123, 1979.

[39] V. Baluni, *CP-nonconserving effects in quantum chromodynamics*, Phys. Rev. D**19**, p. 2227, 1979.

[40] M. Pospelov, A. Ritz, *Theta Vacua, QCD Sum Rules, and the Neutron Electric Dipole Moment*. arXiv:hep-ph/9908508v4, 2005.

[41] C. A. Baker, D. D. Doyle, P. Geltenbort, K. Green, M. G. D. van der Grinten, P. G. Harris, P. Iaydjiev, S. N. Ivanov, D. J. R. May, J. M. Pendlebury, J. D. Richardson, D. Shiers, K. F. Smith, *An Improved Experimental Limit on the Electric Dipole Moment of the Neutron*. arXiv:hep-ex/0602020v3, 2006.

[42] P. G. Harris, C. A. Baker, K. Green, P. Iaydjiev and S. Ivanov, *New Experimental Limit on the Electric Dipole Moment of the Neutron*. Phys. Rev. Lett **82**, pp. 904–907, 1999.

[43] R. D. Peccei, H. R. Quinn, *CP Conservation in the Presence of Pseudoparticles*. Phys. Rev. Lett. **38**, pp. 1440–1443, 1977.

[44] R. D. Peccei, H. R. Quinn, *Constraints imposed by CP conservation in the presence of pseudoparticles*. Phys. Rev. **D**16, pp. 1791–1797, 1977.

[45] M. A. B. Bg, H. -S. Tsao, *Strong P and T Noninvariances in a Superweak Theory*. Phys. Rev. Lett. **41**, p. 283, 1978.

[46] H. Georgi, S. L. Glashow, *Soft Superweak CP Violation and the Strong CP Puzzle*. arXiv:hep-ph/9807399v4, 1999.

[47] F. Wilczek, *Problem of Strong P and T Invariance in the Presence of Instantons*. Phys. Rev. Lett. **40**, p. 279, 1978.

[48] S. Weinberg, *A New Light Boson?* Phys. Rev. Lett. **40**, p. 223, 1978.

[49] F. Wilczek, *The Birth of Axions*. Current Contents **22**, #16, p. 8, 1991. URL: `http://www.garfield.library.upenn.edu/classics1991/A1991FE76900001.pdf`

[50] K. Nakamura et al. (Particle Data Group), *Axions and other similar particles*. JPG **37**, 075021, 2010.

[51] J. E. Kim, *Weak-Interaction Singlet and Strong CP Invariance*. Phys. Rev. Lett. **43**, pp. 103–107 , 1979.d

[52] M.A. Shifman, A.I. Vainshtein, V.I. Zakharov, *Can confinement ensure natural CP invariance of strong interactions?*. Nuc. Phys. B**166**, pp. 493–506, 1980.

[53] W.A. Bardeen, S.-H.H. Tye, J.A.M. Vermaseren, *Phenomenology of the new light Higgs boson search*. Phys. Lett. B**76**, p. 580, 1978.

[54] W.A Bardeen, R.D. Peccei, T. Yanagida, *Constraints on variant axion models*. Nucl. Phys. B **279**, p. 401, 1987.

[55] A.R. Zhitnitsky, *On Possible Suppression of the Axion Hadron Interactions*. Sov. J. Nucl. Phys. **31**, p. 260, 1980.

[56] M. Dine, W. Fischler, M. Srednicki, *A simple solution to the strong CP problem with a harmless axion*. Phys. Lett. B **104**, p. 199, 1981.

[57] T. Goldman, C. M. Hoffman, *Will the axion be found soon?* Phys. Rev. Lett. **40** pp. 220–222, 1978.

[58] J.-M. Frère, M.B. Gavela, J.A.M Vermaseren, *The elusive axion*. Phys. Lett. B**103** p. 129, 1981.

[59] M. B. Wise, *Radiatively-induced flavor-changing neutral Higgs-boson couplings*. Phys. Lett. B**103** p. 121, 1981.

[60] K. van Bibber, N.R. Dagdeviren, S.E. Koonin, A.K. Kerman, H.N. Nelson, *Proposed Experiment to Produce and Detect Light Pseudoscalars*. Phys. Rev. Lett. **59**, p. 759, 1987.

[61] The ALPS Collaboration, *New ALPS results on hidden-sector lightweights*. Phys. Lett. B**689** pp. 149–155, 2010.

[62] L. Maiani, R. Petronzio, E. Zavattini, *Effects of nearly massless, spin-zero particles on light propagation in a magnetic field*. Phys. Lett. B**175**, pp. 359–363, 1986.

[63] Y. Semertzidis et al., *Limits on the Production of Light Scalar and Pseudoscalar Particles*. Phys. Rev. Lett. **64**, p. 2988, 1990.

[64] The PVLAS Collaboration, *Experimental Observation of Optical Rotation Generated in Vacuum by a Magnetic Field*. Phys. Rev. Lett. **96** 110406, 1990.

[65] The PVLAS Collaboration, *New PVLAS results and limits on magnetically induced optical rotation and ellipticity in vacuum*. Phys. Rev. D**77** 032006, 1990.

[66] H. Primakoff, *Photo-production of neutral mesons in nuclear electric fields and the mean life of the neutral meson*. Phys. Rev. **81**, p. 899, 1951.

[67] The CAST Collaboration, *An improved limit on the axion-photon coupling from the CAST experiment*. JCAP **0704** 010, 2007.

[68] G. G. Raffelt, *Astrophysical Axion Bounds*. Lect. Notes Phys. **741**, 51, 2008.

[69] The SNO Collaboration, *Independent Measurement of the Total Active* ^8B *Solar Neutrino Flux Using an Array of* ^3He *Proportional Counters at the Sudbury Neutrino Observatory*. Phys. Rev. Lett. **101** 110301, 2008.

[70] P. Gondolo, G. G. Raffelt, *Solar neutrino limit on axions and keV-mass bosons*. Phys. Rev. D**79** 107301, 2009.

[71] G. G. Raffelt, *Stars as Laboratories for Fundamental Physics*. University of Chicago Press, 1996.

[72] The CAST experiment, `http://cast.web.cern.ch/CAST/`

[73] K. Barth, *et. al.*, *CAST constraints on the axion-electron coupling*. arXiv:1302.6283v2 [astro-ph.SR], 2013.

[74] The CAST Collaboration, *Search for Sub-eV Mass Solar Axions by the CERN Axion Solar Telescope with* ^3He *Buffer Gas*. Phys. Rev. Lett. **107** 261302, 2011.

[75] The Planck Collaboration, *Planck 2013 results. XVI. Cosmological parameters*. arXiv:1303.5076v1 [astro-ph.CO], 2013.

[76] J. Simon, M. Geha, *The Kinematics of the Ultra-Faint Milky Way Satellites: Solving the Missing Satellite Problem*. arXiv:0706.0516v2 [astro-ph], 2007.

[77] P. Tisserand et al., *Limits on the Macho Content of the Galactic Halo from the EROS-2 Survey of the Magellanic Clouds*. arXiv:astro-ph/0607207v2, 2007.

[78] M. Lovell et al., *The haloes of bright satellite galaxies in a warm dark matter universe*. arXiv:1104.2929v2 [astro-ph.CO], 2011.

[79] F. Steffen, *Gravitino Dark Matter and Cosmological Constraints*. arXiv:hep-ph/0605306v2, 2006.

[80] J. Stasielak, P. Biermann, A. Kusenko, *Thermal evolution of the primordial clouds in warm dark matter models with keV sterile neutrinos*. arXiv:astro-ph/0606435v3, 2006.

[81] M. Viel et al., *Can sterile neutrinos be ruled out as warm dark matter candidates?*. arXiv:astro-ph/0605706v2, 2006.

[82] M. Turner, *Early-Universe Thermal Production of Not-So-Invisible Axions*. Phys. Rev. Lett. **59**, p. 2489, 1987.

[83] J. Kim, G. Carosi, *Axions and the Strong CP Problem*. arXiv:0807.3125v2, 2008.

[84] S. Hannestad, A. Mirizzi, G. Rafffelt, *New cosmological mass limit on thermal relic axions*. arXiv:hep-ph/0504059v1, 2005.

[85] M. Archidiacono, S. Hannestad, A. Mirizzi, G. Rafffelt, Y. Wong, *Axion hot dark matter bounds after Planck*. arXiv:1307.0615v1 [astro-ph.CO], 2013.

[86] T. Moroi, H. Murayama, *Axionic Hot Dark Matter in the Hadronic Axion Window*. arXiv:hep-ph/9804291v3, 1998.

[87] D. Grin, G. Covone, J.-P. Kneib, M. Kamionkowski, A. Blain, E. Jullo, *A Telescope Search for Decaying Relic Axions*. arXiv:astro-ph/0611502v2, 2006.

[88] E. Massó, R. Toldrà, *New Constraints on a Light Spinless Particle Coupled to Photons*. arXiv:hep-ph/9702275v1, 1997.

[89] J. Preskill, M. Wise, F. Wilczek, *Cosmology of the invisible axion*. Phys. Lett. B**120**, p. 127, 1983.

[90] L. Abbott, P. Sikivie, *A cosmological bound on the invisible axion*. Phys. Lett. B**120**, p. 133, 1983.

[91] M. Dine, W. Fischler, *The not-so-harmless axion*. Phys. Lett. B**120**, p. 137, 1983.

[92] D. Gross, R. Pisarski, L. Yaffe, *QCD and instantons at finite temperature*. Rev. Mod. Phys. **53**, p. 43, 1981.

[93] L. Duffy, K. van Bibber, *Axions as Dark Matter Particles*. arXiv:0904.3346v1 [hep-ph], 2009.

[94] S. Chang, C. Hagmann, P. Sikivie, *Studies of the Motion and Decay of AxionWalls Bounded by Strings*. Phys. Rev. D**59**, 023505, 1999.

[95] P. Sikivie, *Axion Cosmology*. arXiv:astro-ph/0610440v2, 2006.

[96] O. Wantz, E. Shellard, *Axion Cosmology Revisited*. arXiv:0910.1066v3 [astro-ph.CO], 2011.

[97] T. Hiramatsu, M. Kawasaki, K. Saikawa, T. Sekiguchi, *Production of dark matter axions from collapse of string-wall systems*. arXiv:1202.5851v3 [hep-ph], 2012.

[98] E. Kolb, I. Tkachev, *Femtolensing and Picolensing by Axion Miniclusters*. arXiv:astro-ph/9510043, 1995.

[99] The ADMX experiment, `http://www.phys.washington.edu/groups/admx/home.html`.

[100] S. Asztalos et al., *A SQUID-based microwave cavity search for dark-matter axions*. arXiv:0910.5914v1 [astro-ph.CO], 2009.

[101] S. Asztalos et al., *Design and performance of the ADMX SQUID-based microwave receiver*. Nuclear Instruments and Methods in Physics A **656**, pp. 39–44, 2011.

[102] P. Brun, D. Wouters, *Constraints on axion-like particles with H.E.S.S. from observations of PKS 2155-304*. arXiv:1307.6068v1 [astro-ph.HE], 2013.

[103] The E949 Collaboration, *Measurement of the $K^+ \to \pi^+ \nu\bar{\nu}$ Branching Ratio*. arXiv:0709.1000v2 [hep-ex], 2008.